BRAIN and NERVE 60(2) : 115-121, 2008

特 集　がん治療と神経障害

BRAIN and NERVE

放射線照射による脊髄障害と神経叢障害

Radiation Myelopathy and Plexopathy

嶋 崎 晴 雄*　中 野 今 治*

Haruo Shimazaki, Imaharu Nakano

Abstract

Radiation myelopathy (RM) is a relatively rare disorder characterized by white matter lesions of the spinal cord resulting from irradiation. It is divided into two forms by the latent periods: transient RM and delayed RM. The delayed RM develops usually non-transverse myelopathy symptoms such as dissociated sensory disturbance, unilateral leg weakness, and gait disturbance with asymmetric steps. Spinal MRI shows initially cord swelling and long T_1／T_2 intramedullary lesion with enhancement, then exhibits cord atrophy. Histopathological findings of delayed RM are white matter necrosis, demyelination, venous wall thickening and hyalinization. Glial theory and vascular hypothesis have been proposed to explain its pathophysiology. Several therapies such as adrenocorticosteroid, anticoagulation and hyperbaric oxygen have been tried to this disease with variable benefits.

Radiation plexopathy is classified into two major types by the location: radiation-induced brachial plexopathy (BP) and radiation-induced lumbosacral plexopathy (LSP). The BP initially emerges as arm and shoulder pain, whereas LSP as leg weakness. Myokymia and fasciculations are observed in both types. Electrophysiological study reveals findings of peripheral neuropathy. It is often difficult to distinguish the radiation plexopathy from cancer invasion to the plexus, but MRI is useful to differentiate between these diseases. Pathological findings are small vessel obstruction, thick fibrosis, axonal degeneration and demyelination. Its pathomechanism is presumed that radiation-induced fibrous tissue compresses the nerve root as well as microvascular obstruction of the nerve. Adrenocorticosteroid and anticoagulation are considered as the strategy for symptomatic relief.

Key words : delayed radiation myelopathy, chronic progressive radiation myelopathy, radiation-induced brachial plexopathy (BP), radiation-induced lumbosacral plexopathy (LSP)

Ⅰ．放射線神経障害

がん治療のため放射線照射を行った場合，それが原因で神経系に障害をきたすことがある。神経系の放射線障害は，その神経障害部位から放射線脳障害，放射線脊髄症，放射線末梢神経障害に大きく分けられる。また，障害の経過からは，放射線照射後数日から数カ月して起こり，一過性で1～9カ月（平均3カ月）で自然寛解する急性一過性放射線障害と，照射後6カ月以降に生じる難治性の慢性進行性放射線神経障害に分類される[1]。本稿では，主として遅発性放射線脊髄障害と，末梢神経障害について概説する。

Ⅱ．遅発性放射線脊髄症 (delayed radiation myelopathy: DRM)

DRMは慢性進行性放射線脊髄症（chronic progressive radiation myelopathy）とも呼ばれ，放射線照射終了後，1年前後が最も多いが，数カ月から数年後に脊髄症状が現れ，一般に予後不良である。

DRMは，放射線照射を受けた患者の数パーセントに

* 自治医科大学内科学講座神経内科学部門〔〒329-0498　栃木県下野市薬師寺3311-1〕Division of Neurology, Department of Internal Medicine, Jichi Medical University, 3311-1 Yakushiji, Shimotsuke, Tochigi 329-0498, Japan

1881-6096/08/¥500/論文/JCLS

Fig. 1　遅発性放射線ミエロパチー
脊髄全体が高度に障害され，壊死（星印）の部分が認められる。第3頸髄（上：KB染色，下：HE染色，×5）。

Fig. 2　Fig. 1の壊死部の拡大
壊死部にはコレステリン結晶が沈着し，周囲にはマクロファージが浸潤している（HE染色，×100）。

発症すると推測されている。その発症には，総線量のみでなく，1回照射量，照射される脊髄の長さ，照射期間，照射感覚とも関連している。総線量の安全限界は35～40 Gyとみなされている[2]。57～61 Gyでは5％，68～73 Gyでは50％の率でradiation myelopathyを発症したとの報告がある[5]。

1．臨床症状

異常感覚で発症することが多く，手足のしびれ感やピリピリ感を訴える。多くの場合，その初期には下肢から始まる解離性感覚障害（温痛覚が侵され，触覚は保たれる），ならびに下肢の脱力や歩行障害が現れる。Lhermitte徴候を伴うことも少なくない。初めから左右対称性に障害されることもあるが，通常一側性である。しかし進行すると両側性となることが多い。

症状は徐々に進行する。病変が進行すれば他の他覚的神経所見も認められるようになる。痙性対麻痺を呈し，下肢の腱反射亢進，病的反射陽性となる。また障害部以下の全感覚の低下，消失がみられる。中でも深部感覚障害が目立つことが多く，そのため感覚性運動失調が認められる。

2．検査所見

脳脊髄液検査では一般的に正常だが，蛋白とリンパ球，ミエリン塩基性蛋白の軽度増加を認めることがある。

通常，画像診断では単純X線写真，骨シンチ，脊椎CTは異常はみられないが，他疾患との鑑別に役立つ。ミエログラフィーも異常を呈さないことが多いが，時として脊髄の腫大がみられることがある[4]。MRIは最も診断に寄与すると考えられる。Wangらの10症例の検討[3]では，発症から8カ月以内の場合，T_1強調で低信号，T_2強調で高信号の長い脊髄病変がみられ，約半数でgadoliniumにenhanceされた。この時期では脊髄腫大は稀ではない。一方，発症から3年以上経った症例では，信号異常はなく，萎縮した脊髄が描出されたという[3]。照射を受けて8年後に発症し，その11カ月後に胸髄に空洞形成がみられた例の報告もある[5]。また，放射線により赤色髄が脂肪に置換されるために，照射野の椎体はT_1強調像で高信号に，T_2強調像で中間信号になることも参考になるという[6]。一方，発症後8年で，FDP-PETで頸髄病変のグルコース代謝の亢進を捉えた報告もある[7]。その原因は，炎症ではなく，病変部位で神経活動電位を起こすためのエネルギー需要が増加しているためと推定されている。

電気生理学的検査は，診断には有用でないと報告されている[8]。

3．病理

病変は照射範囲内の脊髄節に限られ，照射中央部の変化が最も強い。病変は通常左右非対称で，灰白質より白質が，前索よりも側索や後索が侵されやすく，壊死部がみられる（Fig. 1）。壊死部にはコレステリン結晶が沈着し，周囲にはマクロファージが浸潤している（Fig. 2）。毛細血管内皮細胞の障害に基づく血行障害性壊死が主体と考えられている。主病変は静脈で，静脈壁は肥厚し著しいヒアリン化を認め（Fig. 3），線維素血栓がみられ，白質神経線維の消失，小動脈の閉塞もみられる。

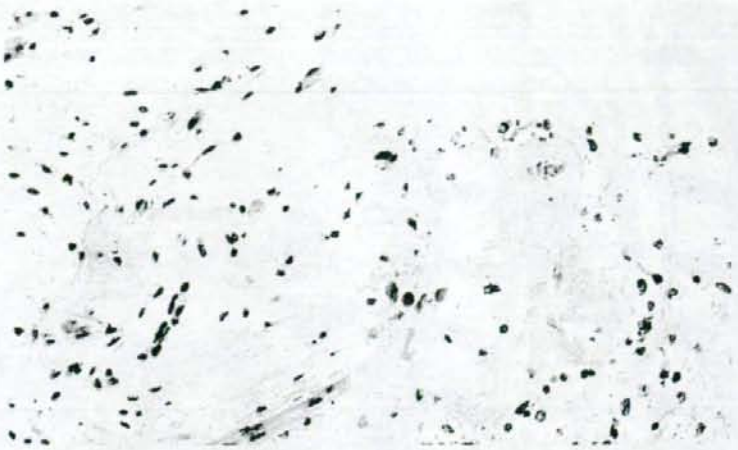

Fig. 3　壁が肥厚してヒアリン化した血管（HE 染色，×200）。

4．病態機序

種々の仮説があるが，古典的には glial theory と vascular hypothesis が提唱されている[9]。

グリア説は，グリア，特にオリゴデンドロサイトの DNA が放射線により障害され，有糸分裂の際に細胞死に陥り，白質が破壊される原因となっているとするものである。しかし，オリゴデンドロサイトはゆっくりとしか分裂しないので，それだけで大きな脱髄巣や白質病変はきたしにくいのではないかという反論もある。さらに，オリゴデンドロサイトは白質に均一に分布しているが，放射線脊髄障害の白質病変は，ある部位に限局しており，その周囲に障害のない白質で取り囲まれているという事実も説明できない。

一方，血管説は，放射線による血管障害により循環障害が生じ，二次的に白質病変を生じるとするものである。血管運動神経の刺激や，血管内皮の炎症による閉塞もメカニズムとして推定されているが，血管透過性の亢進が重要であるとする報告が多い。中枢神経にのみ病変が生じることも，そこの血管が選択的に中性子を捕獲する特徴をもつことで説明できるという[10]。しかし，白質病変部位の血管に形態学的な異常がみられない例も存在するという反証もある[11]。形態の異常がみられない血管においても，照射後血管内皮に作用する，いくつかのサイトカインの濃度に変化がみられたとの報告もある[11]。現在では，2つの機序が両者とも放射線脊髄症の病変形成に関与しているという見方が一般的になっている。

5．診断，鑑別診断

放射線脊髄症の診断基準として，以下の3点を満たすことが必要である[12]。

1）脊髄が放射線照射野に含まれている。

2）神経学的障害が放射線照射を受けた脊髄髄節に対応している。

3）転移あるいは他の原発性脊髄病変が除外される。

鑑別診断としては，原疾患の脊髄転移や，壊死性がん性脊髄症が最も重要であるが，その他の進行性の脊髄症（髄内腫瘍，傍腫瘍性症候群，運動ニューロン疾患）などが鑑別の対象となる。

6．治療，予後

根治療法は現在のところないが，浮腫や炎症の存在と関連して，短期間のステロイド投与が有効であった患者も存在する。ステロイド漸減で症状が急速に悪化した症例[4,13]もあるが，再燃を示さず治癒したと考えられる例もある[14,15]。ステロイドが一定期間有効であっても，その後に症状が進行した報告もある[16]。

ステロイドが無効で，ヘパリン・ワーファリンによる抗凝固療法後に症状の進行停止や[17]，軽快がみられたとの報告がある[18]。有効であった機序としては，小血管内皮の損傷進行を停止し，回復させたと推測している。

高圧酸素療法を行った9例中6例で，症状が進行停止あるいは改善したとの報告がある[19]。また，放射線脊髄症の発症が予測されるケースでは，予防的に高圧酸素療法を勧める意見もある[20]。高圧酸素療法は，照射を受けた組織の血管新生を促し，遅発性放射線障害を軽減すると考えられている。

上記のような治療有効例もあるが，一般的には神経症状は数週から数カ月間にわたり緩徐に進行し，不可逆的

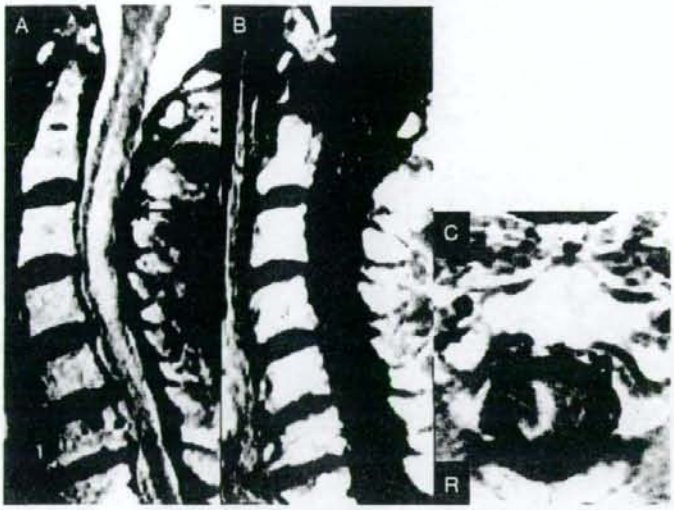

Fig. 4　遅発性放射線脊髄症の頸髄 MRI
(自験例，文献 21 と同例)
A：T_2 強調像矢状断：C1-4 椎体後方の頸髄内に高信号域(矢印)を認め，頸髄は腫脹していた。B，C：Gd 造影 T_1 強調像：C1-2 椎体後方の頸髄右側にリング状の増強効果（矢頭）を認めた。C 2，3 の椎体の信号は T_1 強調で高信号(B)，T_2 強調で中間から高信号（A）となっており（A，B 細矢印），放射線照射による脂肪髄化が示唆される。

とされる[12]。

7．自験例[21]

〈症　例〉56 歳，女性

1991 年 5 月，上咽頭腫瘍にて化学療法および放射線療法(60 Gy)を施行した。1996 年 2 月中旬より左大腿の異常感覚が出現し，翌日には左下肢の温度覚が消失した。2 月末頃から右上肢の筋力低下を自覚し，3 月上旬には右下肢の筋力低下，翌日に排尿困難が出現し，5 日後に当科入院となった。

入院時の神経学的所見では，右上下肢不全麻痺と深部腱反射亢進，左C 5 以下の温痛覚低下，排尿障害が認められ，Brown-Séquard 症候群を呈していた。頸髄 MRI T_2 強調像矢状断（Fig. 4 A）では，C1-4 椎体後方の頸髄内に高信号域を認め，頸髄は腫脹していた。Gd 造影 T_1 強調像（Fig. 4 B，C）では，C1-2 椎体後方の頸髄右側にリング状の増強効果を認めた。減圧目的で C1-2 laminectomy を施行した。術中のエコーでは腫瘍を示唆する所見はみられなかった。ステロイドや抗凝固療法を行ったが，症状は徐々に進行した。

III．放射線神経叢障害

末梢神経は生体組織の中で極めて放射線感受性が低く，放射線障害は生じにくいとされている。総線量と末梢神経障害発症率の関連については，58 Gy 照射された患者の 15%，63 Gy 照射を受けた患者の 75%に発症したと報告されている[22]。放射線照射から症状発症までの期間は平均 4 年間で，3 カ月から 26 年間と幅がある。60 Gy 以上照射を受けた場合，照射後 1 年以内に発症するのに対し，60 Gy 以下の場合，1 年以上経ってから症状が出現するとされている[23]。長い潜伏期間は末梢神経の放射線抵抗性の強いことを示している。放射線末梢神経障害は主として，乳がんなどの治療後に生じる radiation-induced brachial plexopathy と，骨盤腔腫瘍に対する治療に伴い生じる，radiation-induced lumbosacral plexopathy に分類されている。

1．臨床症状

Radiation-induced brachial plexopathy での初発症状は，一側性の腕や肩の痛みが多く，照射部位の神経領域に一致した異常感覚や感覚低下，深部腱反射の低下を認め，数カ月後に脱力が明らかになることが多い。また fasciculation，myokymia が特徴的とされる[1]。Radiation-induced lumbosacral plexopathy は，照射部位から 3 つのタイプに分類される[24]。①子宮や膀胱，直腸がんに対しての骨盤腔，後壁照射による仙骨神経叢障害，②鼠径リンパ節の照射による大腿神経障害，③傍大動脈リンパ節照射による腰神経叢障害，である。最も多いのは仙骨神経叢と大腿神経が障害されるタイプである。症状は下肢の脱力が主で，感覚障害は比較的軽度である。そのため，post-irradiation lower motor syndrome と呼ばれることもある[25]。Brachial plexopathy とは対称的に，痛みは伴わないことが多く，下肢に痛みが放散する患者をみた場合は，まず，がんの再発や浸潤を考えたほうがよいとされる。その他，持続性の fasciculation や

myokymia，腱反射低下などを呈するが，膀胱直腸障害はみられない[24]。

2．検査所見

髄液検査では軽度の蛋白上昇を認めることがある。末梢神経伝導検査では，運動神経は CMAP (componud muscle action potentials) の低下，MCV (motor nerve conduction delocity)，F 波潜時の遅延または消失，plexus の近位と遠位間での conduction block，SNAP (sensong nerve action potentials) 低下が多くみられる[24]。針筋電図では障害部位に一致して限局性，慢性の部分的脱神経と再支配を示す所見，傍脊柱筋の fibrillation や，myokymic discharge が認められる[26,27]。

Lumbosacral plexopathy 例での腓腹神経生検では，軸索変性による著明な有髄線維変性，大径および小径線維の減少がみられたとの報告がある[28,29]。

MRI では，radiation-induced brachial plexopathy 例での放射線による線維化を描出できるが，T_2 強調像では低信号または高信号であり，造影されることもある[30]。Radiation-induced lumbosacral plexopathy の MRI 所見として，馬尾前面の線状の増強効果[25,31,32]や粒状の増強効果[33]を認めた報告がなされている。

3．病理

形態学的変化は，壊死，小動脈の中膜ヒアリン化，神経線維の線維性組織への置換，脱髄，神経周囲膜の肥厚などである[34]。Radiation-induced lumbosacral plexopathy をきたした剖検例では，神経根周囲の細血管障害，血管内皮障害や馬尾神経根の軸索変性，脱髄，神経鞘の菲薄化などがみられ，前角細胞に central chromatolysis が認められた[35]。

4．病態機序

遅発性放射線末梢神経障害の発症機序としては，以下のものが考えられている。まず，神経周囲の組織の線維化による機械的圧迫によるとするもの[22]，また，放射線照射によりサイトカインやフリーラジカルが活性化され凝固能が亢進し，血管内皮障害が生じ，末梢神経の細血管障害や脱髄を起こしているとする可能性が考えられている[36]。さらに，Schwann cell または axon 自体への直接影響[37]，schwannoma，neurinoma，sarcoma などの発生によるとする報告[38,39]がある。

5．診断，鑑別診断

診断に際しては，放射線照射歴，照射部位，発症までの期間などが参考になるが，腫瘍の浸潤による plexopathy が主な鑑別疾患であり，実地臨床上鑑別困難なことがある。Radiation-induced brachial plexopathy を考えさせる所見としては，①腕神経叢の upper trunk (C5-6) の障害 (lower trunk は鎖骨で照射より保護されるため[40])，②痛みでなく異常感覚で発症する，③リンパ浮腫がある，④皮膚に放射線照射による変化がある，⑤線量が 60 Gy 以上であることである[23]。また，radiation-induced lumbosacral plexopathy を支持する所見としては，両下肢の脱力が多く，痛みや感覚障害がないことが挙げられる[41]。両者に共通する鑑別点として，筋電図での障害部位の myokymic discharge はがん転移ではみられにくいとの報告がある[27]。病変部の CT または MRI を撮影すれば腫瘍再発の確認に役立つ[42]。さらに，brachial plexus 周囲の生検により，病理組織学的に検討し，1 本の神経束を取り囲む緻密な線維性結合組織がみられた報告がある[43]。その他の鑑別疾患として，radiation-induced brachial plexopathy では，外傷，局所の感染，SLE，PN などの膠原病による神経血管障害による局所の血栓などがあり，radiation-induced lumbosacral plexopathy では，大動脈瘤，腸腰筋膿瘍などの圧迫，diabetic amyotrophy，産科的処置による障害などがある[1]。

6．治療，予後

ステロイド大量療法が有効であった例[44]，デポ型ステロイド局部注射が一過性に有効であった例[45]，放射線神経叢障害で副腎皮質ステロイドが無効であった例に，抗凝固療法を行い，症状改善に有効であった症例[18]や，conduction block も改善した症例[46]，副腎皮質ステロイドとワーファリンの併用療法を行い，著効した例[31,32]の報告もあるが，副腎皮質ステロイドの漸減中に増悪した例や，無効の例[4,13,18]も存在する。また，疼痛に対して内服が無効な 8 例の brachial plexopathy 例に対し，頸髄後根の entry zone を電気凝固することで疼痛を緩和できたとの報告もある[47]。

治療奏効例の報告もあるが，一般に本症の予後は不良で，lumbosacral plexopathy では，発症後 6 カ月～7 年の経過で，17 例中 12 例が悪化，4 例が不変，改善 1 例と報告されている[41]。

7．自験例

〈症　例〉 49 歳，男性

1979 年 7 月中旬に他院にて右精巣 seminoma を摘出し，その後両側鼠径部，腸骨動脈および傍大動脈 (L1 の

レベルまで)を照射野として，合計120 Gyの放射線照射を受けた。1982年1月頃より，右足が段差につまずいたり，階段から下りるとき右足で体重を支えられなくなった。8月に当科外来を受診した。両大腿部の知覚低下を指摘された。その後も右足の筋力低下は少しずつ増悪し，階段は手すりを使わないと上り下りができなくなったため，1984年10月上旬，当科に第1回目の入院となった。

入院時の所見では，下腹部両側腸骨動脈部から鼠径部にかけて，逆V字型に褐色の放射線皮膚炎の瘢痕が認められた。神経学的には右に強い両側腸腰筋と大腿四頭筋の筋力低下と，両側膝蓋腱反射の消失を認めた。下肢の病的反射や膀胱直腸障害はなく，右大腿内側の痛覚と触覚の軽度低下を認めた。大腿神経のMCVは，右が34.0 m/s，左が42.2 m/sと低下していた。針筋電図では左大腿四頭筋に高振幅のunitが認められた。腰椎ミエログラフィーは異常なく，radiation neuropathyと診断した。退院後，通院を自己中断していたが，下肢の筋力低下が進行したため1999年8月に再受診し，10月下旬に当科に第2回目の入院となった。入院時には，両側大腿前面の筋萎縮が著明で，両側腸腰筋，大腿四頭筋，縫工筋，大腿内転筋，中小殿筋，右腓骨筋の筋力低下を認めた。両側膝蓋腱とアキレス腱反射は消失していた。痛覚は右大腿内側で低下していた。今回は右の総腓骨神経のMCVも34.7 m/sと低下していた。針筋電図では右前脛骨筋にも神経原性変化が認められた。Radiation-induced lumbosacral plexopathyと診断し，プレドニゾロン40 mg/dayの内服を開始し，軽度の筋力回復がみられた。

文　献

1) 佐竹真理恵, 橋口良也, 法化図陽一, 永松啓爾: 放射性神経障害. 日本臨牀 別冊 神経症候群V, その他の神経疾患, 東京, 2000, pp563-568
2) 中野今治: ミエロパチー. 神経内科学書, 第1版, 豊倉康夫(編), 朝倉書店, 東京, 1987, pp844-851
3) Wang PY, Shen WC, Jan JS: MR imaging in radiation myelopathy. AJNR Am J Neuroradiol **13**: 1049-1055, 1992
4) Worthington BS: Diffuse cord enlargement in radiation myelopathy. Clin Radiol **30**: 117-119, 1979
5) 新藤和雅, 新田清明, 網野章由, 長坂高村, 塩澤全司: 胸髄に空洞形成のみられた慢性進行性放射線脊髄症の1例. 臨床神経 **35**: 1012-1015, 1995
6) 柳下 章: 放射線脊髄症. 脊椎脊髄疾患のMRI, 柳下 章(編), 三輪書店, 東京, 2004, pp257-258
7) Esik O, Emri M, Csornai M, Kasler M, Godeny M, et al: Radiation myelopathy with partial functional recovery: PET evidence of long-term increased metabolic activity of the spinal cord. J Neurol Sci **163**: 39-43, 1999
8) Rampling R, Symonds P: Radiation myelopathy. Curr Opin Neurol **11**: 627-632, 1998
9) Okada S, Okeda R: Pathology of radiation myelopathy. Neuropathology **21**: 247-265, 2001
10) Morris GM, Coderre JA, Bywaters A, Whitehouse E, Hopewell JW: Boron neutron capture irradiation of the rat spinal cord: histopathological evidence of a vascular-mediated pathogenesis. Radiat Res **146**: 313-320, 1996
11) Tsao MN, Li YQ, Lu G, Xu Y, Wong CS: Upregulation of vascular endothelial growth factor is associated with radiation-induced blood-spinal cord barrier breakdown. J Neuropathol Exp Neurol **58**: 1051-1060, 1999
12) Goldwein JW: Radiation myelopathy: a review. Med Pediatr Oncol **15**: 89-95, 1987
13) Godwin-Austen RB, Howell DA, Worthington B: Observations on radiation myelopathy. Brain **98**: 557-568, 1975
14) 宇高不可思, 辻 輝之, 重松一生: 副腎皮質ステロイド薬が著効を示したchronic progressive radiation myelopathyの1例. 臨床神経 **30**: 439-443, 1990
15) Berendes K, Dorstelmann D: Radiation myelopathy-two cases with unusual development. J Neurol **216**: 73-76, 1977
16) 広田佐栄子, 副島俊典, 東野貴徳, 大林加代子, 高田佳木, 他: 副腎皮質ステロイド薬の長期投与を行った放射線脊髄症の1例. 臨放 **43**: 649-652, 1998
17) 結城奈津子, 滋賀健介, 山口達之, 中川正法: 抗凝固療法を施行したdelayed radiation myelopathyの1例. 神経内科 **64**: 538-542, 2006
18) Glantz MJ, Burger PC, Friedman AH, Radtke RA, Massey EW, et al: Treatment of radiation-induced nervous system injury with heparin and warfarin. Neurology **44**: 2020-2027, 1994
19) Angibaud G, Ducasse JL, Baille G, Clanet M: Potential value of hyperbaric oxygenation in the treatment of post-radiation myelopathies. Rev Neurol **151**: 661-666, 1995
20) Sminia P, van der Kleij AJ, Carl UM, Feldmeier JJ, Hartmann KA: Prophylactic hyperbaric oxygen treatment and rat spinal cord re-irradiation. Cancer Lett **191**: 59-65, 2003
21) 佐山節子, 中野今治: がんの治療と関連しておこる神経障害－放射線治療と神経障害. Clin Neurosci **15**: 885-887, 1997
22) Stoll B, Andrews J: Radiation-induced peripheral neuropathy. Br Med J **1**: 834-837, 1966
23) Kori SH, Foley KM, Posner JB: Brachial plexus lesions in patients with cancer: 100 cases. Neurology

31: 45-50, 1981
24) Thomas P, Kbernd H: Pheripheral Neuropathy due to physical agent. Peripheral Neuropathy, Dyck PJ, et al (eds), 3rd ed., WB Saunders, Philadelphia, 1993, pp1000-1008
25) Bowen J, Gregory R, Squier M, Donaghy M: The post-irradiation lower motor neuron syndrome neuronopathy or radiculopathy? Brain **119**: 1429-1439, 1996
26) Lederman RJ, Wilbourn AJ: Brachial plexopathy: recurrent cancer or radiation? Neurology **34**: 1331-1335, 1984
27) Harper CM Jr, Thomas JE, Cascino TL, Litchy WJ: Distinction between neoplastic and radiation-induced brachial plexopathy, with emphasis on the role of EMG. Neurology **39**: 502-506, 1989
28) 沼田久美子, 伊藤道子, 内山真一郎, 小林逸郎, 竹宮敏子: 晩発性放射線腰仙部神経叢障害の1例. No to Shinkei **42**: 629-633, 1990
29) 丸山芳一, 法化図陽一, 金久禎秀, 永松啓爾, 大西晃生: 子宮癌に対する骨盤腔内X線照射後にみられた lumbosacral radiation neuropathy の3例. 神経内科 **22**: 52-60, 1985
30) Wouter van Es H, Engelen AM, Witkamp TD, Ramos LM, Feldberg MA: Radiation-induced brachial plexopathy: MR imaging. Skeletal Radiol **26**: 284-288, 1997
31) 姉崎利治, 原田 隆, 河内 泉, 三瓶一弘, 相馬芳明, 他: 副腎皮質ホルモン・ワーファリン併用療法が著効した post-irradiation lumbosacral radiculopathy の1例. 臨床神経 **39**: 825-829, 1999
32) 梅田麻衣子, 成瀬 聡, 伊藤晶子, 藤田信也: 腰髄 MRI で馬尾前面の増強効果をみとめた post-irradiation lumbosacral radiculopathy の1例. 臨床神経 **45**: 758-761, 2005
33) Hsia AW, Katz JS, Hancock SL, Peterson K: Post-irradiation polyradiculopathy mimics leptomeningeal tumor on MRI. Neurology **60**: 1694-1696, 2003
34) Gillette EL, Mahler PA, Powers BE, Gillette SM, Vujaskovic Z: Late radiation injury to muscle and peripheral nerves. Int J Radiat Oncol Biol Phys **31**: 1309-1318, 1995
35) Berlit P, Schwechheimer K: Neuropathological findings in radiation myelopathy of the lumbosacral cord. Eur Neurol **27**: 29-34, 1987
36) Baker DG, Krochak RJ: The response of the microvascular system to radiation: a review. Cancer Invest **7**: 287-294, 1989
37) Lundborg G, Schildt B: Microvascular permeability in irradiated rabbits. Acta Radiol Ther Phys Biol **10**: 311-320, 1971
38) Foley KM, Woodruff JM, Ellis FT, Posner JB: Radiation-induced malignant and atypical peripheral nerve sheath tumors. Ann Neurol **7**: 311-318, 1980
39) Hussussian CJ, Mackinnon SE: Postradiation neural sheath sarcoma of the brachial plexus: a case report. Ann Plast Surg **43**: 313-317, 1999
40) Brennan MJ: Breast cancer recurrence in a patient with a previous history of radiation injury of the brachial plexus: a case report. Arch Phys Med Rehabil **76**: 974-976, 1995
41) Thomas JE, Cascino TL, Earle JD: Differential diagnosis between radiation and tumor plexopathy of the pelvis. Neurology **35**: 1-7, 1985
42) Thyagarajan D, Cascino T, Harms G: Magnetic resonance imaging in brachial plexopathy of cancer. Neurology **45**: 421-427, 1995
43) Gosk J, Rutowski R, Reichert P, Rabczynski J: Radiation-induced brachial plexus neuropathy - aetiopathogenesis, risk factors, differential diagnostics, symptoms and treatment. Folia Neuropathol **45**: 26-30, 2007
44) 法化図陽一, 渡邊 修, 森 敏雄, 永松啓爾, 中村泰也: 乳癌転移巣への放射線治療により radiation neuropathy を発症した1例. 臨床神経 **35**: 211-214, 1995
45) 熊巳真澄, 馬目太三, 山本悌司: Radiation plexopathy に対する methylprednisolone 局注の試み. 神経治療 **15**: 87-89, 1998
46) Soto O: Radiation-induced conduction block: resolution following anticoagulant therapy. Muscle Nerve **31**: 642-645, 2005
47) Teixeira MJ, Fonoff ET, Montenegro MC: Dorsal root entry zone lesions for treatment of pain-related to radiation-induced plexopathy. Spine **32**: E316-319, 2007

お知らせ

本誌は「脳と神経」誌,「神経研究の進歩」誌の統合誌です。雑誌略称は,和文欧文とも「Brain Nerve」になります。

「BRAIN and NERVE」編集室

病　理

中野 今治

筋萎縮性側索硬化症(ALS)には古典型 ALS のほかに家族性 ALS，若年性 ALS，痴呆をともなう ALS など，いくつかのサブタイプがある．本稿のテーマは古典型 ALS (Charcot 病)の病理であり，以降特に断らない限り ALS という術語は古典型 ALS を指すものとする

ALS では上位運動ニューロン(upper motor neuron：UMN)と下位運動ニューロン(lower motor neuron：LMN)が選択的に侵され，それに対応する症候が出現する．実際の病理所見はこの範囲を超えている場合が希でないが，本稿では典型的 ALS の UMN と LMN に絞って述べることにする．

肉眼所見

通常の ALS では，大脳の萎縮はなく，中心前回の萎縮もみられず，大脳の前額断面でも中心溝の内側に位置する中心前回皮質にも萎縮や変色はみられない(図 1)．筆者の経験では，通常は頸髄前根の変色と萎縮が唯一の肉眼所見である．ただし，中心前回の変性が高度の場合にはその萎縮と，前額断面での中心前回皮質の萎縮と変色が認められる(図 2)．

組織所見

1．下位運動ニューロン病変

脊髄では前角が前後方向に萎縮して，その前縁が扁平になり，外側の角が先鋭になる(図 3)．前角の萎縮は，主として前角大型ニューロン(LMN)の脱落(図 4)につれてその樹状突起が消失することによる．

A．LMN 消失への過程

前角の残存ニューロンには正常に見える神経細胞のほかに，種々の細胞病理が観察される．消失に至る過程と考えられる像には，ニッスル小体中心崩壊，細胞体と樹状突起の萎縮，核の偏在化，萎縮した細胞質の赤染化(HE 染色)，リポフスチンによる細胞体占拠(他の細胞質成分が消失した結果)(図 5)，核萎縮と濃縮，神経食作用(neuronophagia)像(図 5)があげられる．

また Golgi 装置に特異的な蛋白(MG-160)に対する抗体を用いて免疫染色を行うと，残存ニューロンの多くが Golgi 装置の断片化を呈している[1]．

ALS における運動ニューロン死はアポトーシスによるとの考えが提唱された[2]が，異論もある[3]．Yamazaki ら[4]は，TdT-mediated dUTP-biotin nick end-labeling (TUNEL)法で ALS 剖検例の脊髄前角細胞を染め，TUNEL法陽性(DNA の断片化が生じていることを示している)あるいは陰性の LMN を写真に撮り，次に HE 染色を施して，撮影しておいたニューロンの HE 染色像を観察した．そうすると TUNEL 法陽性ニューロンは全て高度に萎縮していてかつ核が濃縮しているのに対し，萎縮していないニューロンは TUNEL 法陰性であり，萎縮していても核が明るいニューロンも陰性であった(図 6)．アポトーシス小体は観察されなかった．この所見は，ALS の LMN では DNA の断片化は神経細胞変性の最末期に生じ，アポトーシスとは異なるメカニズムの細胞死が生じている可能性を示している[4]．

B．LMN の異常構造物

1）封入体

残存ニューロンには Bunina 小体(図 7)とユビキチン化した封入体が出現する．

Bunina 小体は好酸性を示す微小な細胞質内封入体(図 7 左)で，ALS に特異的な封入体であるという点で重要である．その構成蛋白や由来は不明であるが，cystatin C，あるいは transferrin に対する抗体で陽性に染まる[5]．電子顕微鏡的には，限界膜を持たず，電子密度の高い顆粒が密に集簇した構造である(図 7 右)．周辺には壊れた膜構造が付着している．内部にしばしば空隙(封入体外の細胞質が陥入したものである可能性がある)を有し，神経細糸や壊れた膜を含んでいるように見える．

ユビキチン陽性封入体には，円形をしたもの(円形封入体)(図 8 左)と，線条に見える封入体(糸束様封入体)(図 8 右)とがある．円形封入体は HE 染色では文字通り丸く見えるが，多くは内部が不規則に網目状に見えて周辺は空胞で囲まれている(図 9 左)．電子顕微鏡的には，神経細糸様の細い線維と異常な太い線維とが混在している構造である(図 9 右上，下)．糸束様封入体の超微形態は，円形封入体内にみられる異常に太い線維のみが束になった構造であり，限界膜はない．糸束様封入体が集簇して円形封入体に移行している像が時に認められる．糸束様封入体はしばしば二重膜を有する小胞で囲繞されており[6]，ユビキチン化の後にリソゾーム系で処理されることが推測される．円形封入体でも同様である．

なかの いまはる　自治医科大学教授/神経内科
0289-0585/08/¥500/論文/JCLS

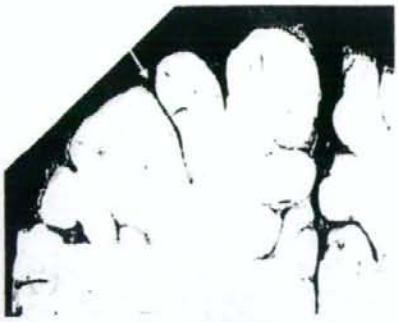

図 1　ALS の中心前回
通常例では中心溝(矢印)の内側に位置する中心前回には萎縮も変色もみられない.

図 3　典型的な ALS 頸髄の横断面
前角が前後方向に萎縮して,その前縁が扁平になり,外側の角が先鋭になる.
KB 染色,約 6 倍

図 4　ALS(上)頸髄前角の大型ニューロンは対照(下)に比して明らかに脱落している.
KB 染色,40 倍

図 5　ALS の腰髄前角
左に萎縮したニューロン,右に神経食細胞像が認められる.
HE 染色

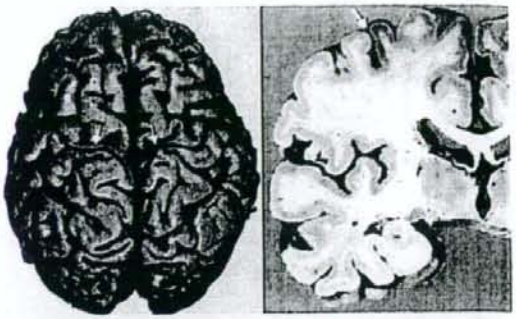

図 2　中心前回の高度萎縮(矢印)を呈する ALS の大脳
前額断面では中心前回に萎縮と変色が認められる.

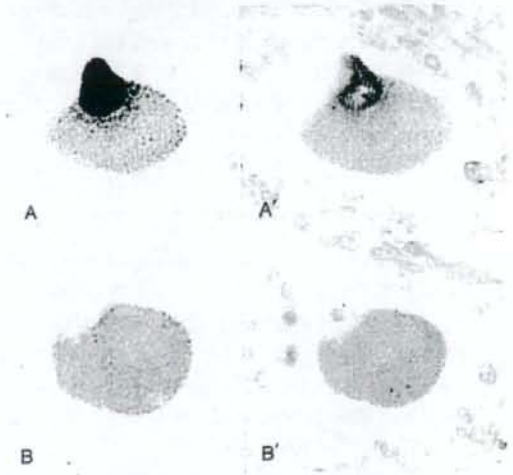

図 6　ALS 前角細胞の TUNEL 法
A と A′,B と B′はそれぞれ同一の細胞である.A,B の細胞とも細胞質は萎縮してリポフスチンで充満しているが,TUNEL 法陽性のニューロン(A)では核が濃縮している(A′)のに対して,陰性のニューロン(B)は明るい核と明瞭な核小体を有している.A,B:TUNEL 法,A′,B′:HE 染色,400 倍

図 7　ALS 前角細胞の Bunina 小体(左:矢印).HE 染色,200 倍.Bunina 小体の電子顕微鏡写真(右).5,000 倍

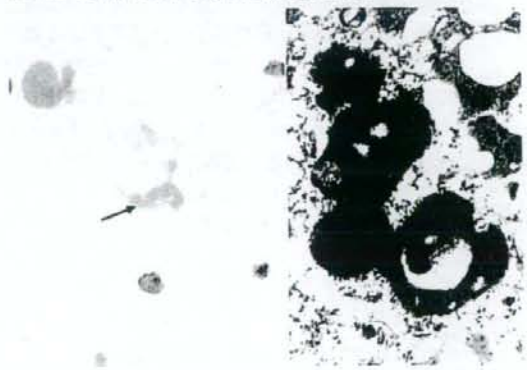

2006 年にこのユビキチン化封入体の構成蛋白が TDP-43 であることが報告され[7,8],大きな注目を集めている.TDP-43 に対する抗体で免疫染色を行うと確かに両者とも陽性に染まる(図 10).

2)スフェロイド

スフェロイドは LMN 軸索近位部に神経細糸が貯留して類球形に腫大した構造である(図 11).早期に死亡した症例で多くみられる.神経細糸は遅い軸索流に関連していることから,ALS の運動ニューロン死には軸索流の障害が

図 8　脊髄前角細胞の円形封入体(左)と糸束様封入体(右)．ユビキチン免疫染色，200 倍

図 9　左)ALS 前角細胞の円形封入体(round inclusion)(星印)，HE 染色，200 倍．**右)円形封入体の電子顕微鏡像**．神経細糸様の細い線維と異常な太い線維とが混在している．右上：2,000 倍，右下：10,000 倍

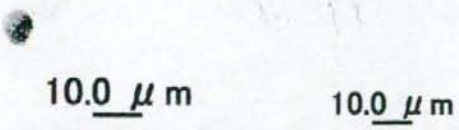

図 10　前角大型ニューロンの円形封入体(左)と糸束様封入体(右)．抗 TDP-43 抗体染色(愛知医科大学加齢医学研究所の橋詰良夫教授，吉田眞理准教授のご好意による)

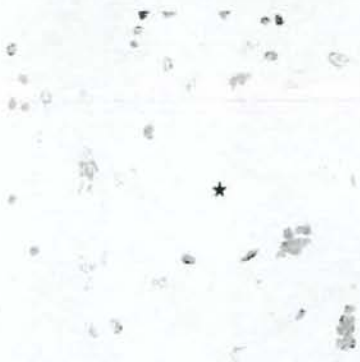

図 11　脊髄前角のスフェロイド(星印)　HE 染色，200 倍

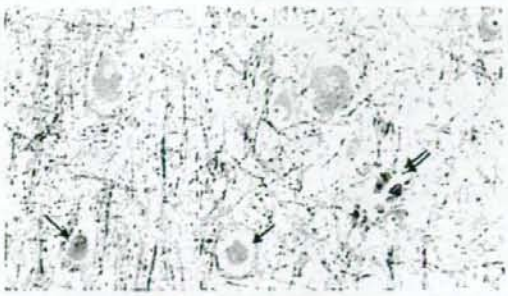

図 12　ALS の細胞の変化
細胞質が均質に染まって萎縮した Betz 細胞(左，右，矢印)や Betz 細胞の消失跡に集簇したマクロファージの像(右，二重矢印)がみられる．KB 染色，200 倍

関係しているとの説もある．

2．上位運動ニューロン病変

上位運動ニューロンの病理像は，LMN ほど精緻には観察されていない．錐体路の淡明化(軸索脱落)(図 3)がしばしば認められる．軸索脱落が軽微な場合は淡明化が捉えにくいので，鍍銀軸索染色で確認する必要がある．

中心前回では，Betz 細胞の変性・萎縮とその消失跡へのマクロファージの集簇(図 12)が認められる．

謝辞：　今回の執筆にあたり，愛知医科大学加齢医学研究所の橋詰良夫教授，吉田眞理准教授より貴重な TDP-43 の免疫染色標本の観察使用を許可いただいた．深い謝意を表する次第である．

文　献

1) Gonatas NK, Stieber A, Mourelatos Z, et al. Fragmentation of the Golgi apparatus of motor neurons in amyotrophic lateral sclerosis. Am J Pathol. 1992；140：731-7.
2) Troost D, Aten J, Morsink F, et al. Apoptosis in amyotrophic lateral sclerosis is not restricted to motor neurons. Bcl-2 expression is increased in unaffected post-central gyrus. Neuropathol Appl Neurobiol. 1995；21：498-504.
3) Migheli A, Cavalla P, Marino S, et al. A study of apoptosis in normal and pathologic nervous tissue after in situ end-labeling of DNA strand breaks. J Neuropathol Exp Neurol. 1994；53：606-16.
4) Yamazaki M, Esumi E, Nakano I. Is motoneuronal cell death in amyotrophic lateral sclerosis apoptosis? Neuropathology. 2005；25：381-7.
5) Mizuno Y, Amari M, Takatama M, et al. Transferrin localizes in Bunina bodies in amyotrophic lateral sclerosis. Acta Neuropathol. 2006；112：597-603.
6) Nakano I, Shibata T, Uesaka Y. On the possibility of autolysosomal processing of skein-like inclusions—electronmicroscopic observation in a case of amyotrophic lateral sclerosis. J Neurol Sci. 1993；120：54-9.
7) Neumann M, Sampathu DM, Kwong LD, et al. Ubiquitinated TDP-43 in frontotemporal lobar degeneration and amyotrophic lateral sclerosis. Science. 2006；314：130-3.
8) Arai T, Hasegawa M, Akiyama H, et al. TDP-43 is a component of ubiquitin-positive tau-negative inclusions in frontotemporal lobar degeneration and amyotrophic lateral sclerosis. Biochem Biophys Res Commun. 2006；35：602-11.

Int. J. Cancer: **120**, 278–284 (2006)

Suppression of ovarian cancer by muscle-mediated expression of soluble VEGFR-1/Flt-1 using adeno-associated virus serotype 1-derived vector

Yuji Takei[1,2], Hiroaki Mizukami[1], Yasushi Saga[2], Ichiro Yoshimura[3], Yoko Hasumi[4], Takeshi Takayama[2], Takahiro Kohno[2], Takashi Matsushita[1], Takashi Okada[1], Akihiro Kume[1], Mitsuaki Suzuki[2] and Keiya Ozawa[1]*

[1]*Division of Genetics Therapeutics, Center for Molecular Medicine, Jichi Medical School, Tochigi, Japan*
[2]*Department of Obstetrics and Gynecology, Jichi Medical School, Tochigi, Japan*
[3]*Department of Urology, National Defense Medical College, Saitama, Japan*
[4]*Department of Obstetrics and Gynecology, University of Tokyo, Tokyo, Japan*

Vascular endothelial growth factor (VEGF) is known to play a major role in angiogenesis in a variety of tumors. A soluble form of Flt-1 (sFlt-1), a VEGF receptor, is potentially useful as an antagonist of VEGF, and accumulating evidences suggest the applicability of sFlt-1 in tumor suppression by means of anti-angiogenesis. We previously demonstrated the efficacy of *sflt-1* gene expression *in situ* to suppress tumor growth and ascites in ovarian cancer. Here, we demonstrate the therapeutic applicability of muscle-mediated expression of sFlt-1 in tumor-bearing mice. Initially, tumor suppressive action was confirmed by inoculating sFlt-1-expressing ovarian cancer (SHIN-3) cells into mice, both subcutaneously and intraperitoneally. To validate the therapeutic efficacy in a more clinically relevant model, adeno-associated virus vectors encoding *sflt-1* were introduced into mouse skeletal muscles and were subsequently inoculated with tumor cells. As a result, high serum sFlt-1 levels were constantly observed, and the growth of both subcutaneously- and intraperitoneally-inoculated tumors was significantly suppressed. No delay in wound healing or adverse events of neuromuscular damage were noted, body weight did not change, and laboratory data, such as those representing liver and renal functions, were not affected. These results indicate that sFlt-1 suppresses growth and peritoneal dissemination of ovarian cancer by the inhibition of angiogenesis, and thus suggest the usefulness of gene therapy for ovarian cancer.

Key words: sFlt-1; AAV; gene therapy; ovarian cancer; VEGF

In recent years, the incidence of ovarian cancer has been on the increase. It is currently the leading cause of death from gynecological cancer.[1] Since the early-stage ovarian cancer is generally asymptomatic, more than half of the patients are diagnosed with the condition at an advanced stage with ascites and peritoneal dissemination.[2] The standard treatment for advanced ovarian cancer is radical cytoreductive surgery followed by combination chemotherapy. Fortunately, ovarian cancer is relatively sensitive to chemotherapy, and a remission can be achieved in a majority of patients, even at the advanced stages.[3,4] Nonetheless, more than half of the patients develop recurrence, and this eventually leads to death, thereby indicating the limitations of the current therapy. Therefore, new strategies are required to improve the therapeutic outcomes.

Angiogenesis is closely related to the development of malignant tumors,[5] and it plays an important role in the growth of primary, metastatic and disseminated lesions of ovarian cancer.[6] Therefore, the inhibition of angiogenesis may suppress peritoneal dissemination, the main mode of progression of ovarian cancer, and may improve the prognosis of advanced ovarian cancer.

The significance of angiogenic factors upon clinical outcome of ovarian cancer have been intensively studied, including vascular endothelial growth factor (VEGF),[7] basic fibroblast growth factor,[8] platelet-derived endothelial cell growth factor (PD-ECGF)[9] and hepatocyte growth factor.[10] Among all, VEGF appears to be the most important and versatile, and it is also reported to be an independent prognostic factor in ovarian cancer patients.[7]

The VEGF-inhibiting factor used in this study was sFlt-1. This is a soluble form of VEGFR-1, and acts as a VEGF antagonist.[11] sFlt-1 is a secretory protein, and systemic expression through circulation can be expected. Main VEGF receptors are Flt-1 and KDR, and both are tyrosine kinase receptors. KDR shows stronger tyrosine kinase activity when the ligand, VEGF, binds, but Flt-1 has stronger VEGF-binding activity.[12,13] Accordingly, when sFlt-1 is present in circulation at a sufficient level, sFlt-1 may competitively inhibit binding of blood VEGF to Flt-1 and KDR, resulting in inhibition of VEGF action.

We have previously demonstrated the tumor suppressive activities of sFlt-1 when it was introduced into ovarian cancer cells.[14] In this study, we aimed at developing a more clinically relevant strategy through a continuous supply of sFlt-1 by muscle-mediated gene transfer using adeno-associated virus (AAV) vectors. AAV vector is derived from a nonpathogenic virus, and a long-term transgene expression can be obtained after intramuscular vector injection.[15–17] Taking these facts into consideration, we began to test the efficacy of the therapeutic approach for ovarian cancer using muscle-mediated *sflt-1* gene expression and compared with the previous strategy which utilized tumor cell transduction.

Material and methods

Cells and plasmids

The human ovarian serous adenocarcinoma cell line SHIN-3[18] was provided by Dr. Y. Kiyozuka (Hyogo College of Medicine, Japan) and used in this study, instead of the previously utilized RMG-1 cells,[14] as the latter cell line did not efficiently form tumors upon inoculation. The SHIN-3 and the human embryonic kidney 293 cell lines were maintained as described previously.[18,19] The murine *sflt-1* cDNA was isolated from the SmaI sites of plasmid psFlt-1[14] and inserted into the SmaI site of the pCMV-IRES-bsr vector[20] to generate pCMV-sFlt-1-IRES-bsr. Luciferase (LUC)-encoding pCMV-LUC-IRES-bsr[20] was used as a control vector. p2ITR-hsFlt-1 is an sFlt-1 expression plasmid prepared by incorporating human *sflt-1* cDNA into the EcoRI site of pAAV-MCS (Stratagene, La Jolla, CA). Suppression of VEGF-driven HUVEC proliferation by conditioned medium of sFlt-1-expressing cells was already confirmed for both murine[14] and human[21] constructs.

Development of stably transduced cells

Either pCMV-sFlt-1-IRES-bsr or pCMV-LUC-IRES-bsr was introduced into the SHIN-3 cells using the standard calcium phosphate precipitation method.[22] After transfection, the cells were cultured and selected in the presence of 10 μg/ml of blasticidin S hydrochloride (Kaken Pharmaceutical, Tokyo, Japan). After 4 weeks, the blasticidin-resistant SHIN-3/sFlt-1 and SHIN-3/LUC

Grant sponsors: Ministry of Health, Labor and Welfare, Japan; Ministry of Education, Culture, Sports, Science and Technology, Japan; Japan Medical Association. The research award to JMS graduate student.

***Correspondence to:** Division of Genetics Therapeutics, Center for Molecular Medicine, Jichi Medical School, 3311-1 Yakushiji, Minamikawachi, Kawachi, Tochigi 329-0498, Japan. E-mail: kozawa@jichi.ac.jp

Received 18 November 2005; Accepted after revision 7 August 2006
DOI 10.1002/ijc.22307
Published online 25 October 2006 in Wiley InterScience (www.interscience.wiley.com).

cell lines were established and maintained thereafter in the presence of 10 μg/ml of blasticidin S hydrochloride.

AAV vector production

AAV vectors were produced based on the triple plasmid transfection to 293 cells using p2ITR-hsFlt-1, the helper plasmid for adenovirus genes,[23] and the helper plasmid for AAV1.[24,25] A plasmid encoding *lacZ* gene was used to prepare the control AAV vector. The vector stocks were purified using iodixanol (Invitrogen, Carlsbad, CA) density-gradient ultracentrifugation,[24,26,27] and the titer was determined by quantitative DNA dot-blot hybridization.

VEGF quantitation

SHIN-3 cells were inoculated into 10-cm dishes and cultured in a 10% FBS-supplemented DMEM medium. When the cells grew to approximately 80% confluence, the culture supernatant was replaced with serum-free culture medium. After 24 hr, the culture supernatant was recovered. The concentration of VEGF in the supernatant was determined by ELISA System (Amersham Biosciences, Piscataway, NJ).

Western blot analysis

sFlt-1 in the culture supernatant of SHIN-3/sFlt-1 was detected by Western blotting, using standard techniques as described previously.[14] Briefly, the culture supernatant was electrophoresed, transferred into nitrocellulose membrane and incubated with a 1:200 dilution of anti-sFlt-1 polyclonal antibody (provided by Dr. Shibuya). Subsequently, the membrane was reacted with a horseradish peroxidase-labeled secondary antibody, *i.e.*, anti-rabbit antibody (Amersham Biosciences). The bound antibody was visualized by chemiluminescence using an ECL kit (Amersham Biosciences).

In vitro *cell growth kinetics*

SHIN-3/sFlt-1 and SHIN-3/LUC were plated in 6-well plates at a density of 5×10^4 cells/well, and cultured in a 10% serum-supplemented DMEM/F-12 medium. For each group, the cells from a single well were dislodged using 0.05% trypsin-EDTA every 24 hr and were counted using a hemocytometer. This experiment was performed in triplicate.

Tumor cell transduction model

Subcutaneously inoculated tumor growth. Four- to five-week-old female BALB/c nude mice (Japan Clea Laboratories, Tokyo, Japan) were used in the experiment. SHIN-3/sFlt-1 or SHIN-3/LUC cells (5×10^6) were subcutaneously transplanted into the back of the mice, and tumor sizes were measured twice a week using a micrometer caliper. The tumor volume was calculated using the formula: volume = (short diameter)^2 × (long diameter) × 0.5.[28]

Angiogenesis in subcutaneous tumor. On the 21st day after the subcutaneous transplantation of 5×10^6 SHIN-3/sFlt-1 or SHIN-3/LUC cells into the back, the mice were killed and the subcutaneous tumors were excised. After fixation of the tumors in 4% paraformaldehyde, frozen sections were cut, and the endogenous peroxidases were blocked with 3% hydrogen peroxide. The sections were incubated overnight at 4°C with a 1:50 dilution of anti-CD31 antibody (Pharmingen, San Diego, CA) as the primary antibody that recognizes vascular endothelial cells. The sections were then reacted with the secondary antibody, *i.e.*, peroxidase-conjugated anti-rat antibody (Simple Stain Mouse MAX-PO, Rat; Nichirei, Tokyo, Japan) at room temperature for 30 min, followed by color development with diaminobenzidine (DAB). In addition to CD31, immunostaining of von Willbrand factor (vWF) and endothelial nitric oxide synthase (eNOS) was performed. For the specific antibodies, anti-vWF (H-300) and anti-NOS3 (C-20) (Santa Cruz Biotechnology, Santa Cruz, CA) were diluted 50 times, and reacted with the sections at room temperature for 2 hr, followed by color development by DAB reaction using a DAKO LSAB Kit (DAKO, Carpinteria, CA). The number of newly formed vessels was counted under a light microscope at 100× magnification.

Ascites and peritoneal tumor dissemination. SHIN-3/sFlt-1 or SHIN-3/LUC cells (5×10^6) were inoculated into mice intraperitoneally. After 23 days, the mice were killed using diethyl ether, the volume of the ascitic fluid was measured and the peritoneally disseminated lesions were weighed. The volume of ascitic fluid was calculated by subtracting 1 ml from the total volume of fluid that was recovered after the intraperitoneal injection of 1 ml of PBS. The weights of the peritoneally disseminated lesions were calculated by subtracting the weight of the intestine of age-matched, untreated mice from the total weight of the intestine and disseminated lesions removed in one block.

Survival time. SHIN-3/sFlt-1 or SHIN-3/LUC cells (5×10^6) were inoculated into mice intraperitoneally, and the mice were monitored twice daily until they died of massive ascites. Survival rates were calculated using the Kaplan–Meier method.

Therapeutic model using AAV vector

Measurement of serum VEGF and ascitic VEGF. Nude mice were subcutaneously ($n = 5$) or intraperitoneally ($n = 5$) inoculated with SHIN-3 cells (5×10^6 cells), and blood was collected from the tail vein 1, 2, and 3 weeks after inoculation. The serum VEGF level was measured using human VEGF ELISA (R&D system, Minneapolis, MN). Mice that received intraperitoneal SHIN-3 cell inoculation were killed using diethyl ether 3 weeks after inoculation ($n = 3$), ascites were collected, and the ascitic VEGF level was measured by ELISA (R&D system).

Measurement of serum sFlt-1. AAV1-sFlt-1 or AAV1-LacZ vector (2.5×10^{12} genome copy) was given in 10 separate injections into the hind limb skeletal muscles of mice, and the blood samples were obtained from the tail vein every 2 weeks. The concentration of sFlt-1 in the serum was measured using a human sVEGF-R1 ELISA (Bender MedSystems, Vienna, Austria).

Subcutaneously inoculated tumor growth. AAV1-sFlt-1 or AAV1-LacZ vector (2.5×10^{12} genome copy) was injected into the hind limb skeletal muscles of mice. After 9 days, the mice were subcutaneously inoculated with 5×10^6 SHIN-3 cells and monitored thereafter.

Peritoneal tumor dissemination. AAV1-sFlt-1 or AAV1-LacZ vector (2.5×10^{12} genome copy) was injected into the hind limb skeletal muscles of mice. After 9 days, the mice were intraperitoneally inoculated with 5×10^6 SHIN-3 cells. After 23 days later, the mice were killed, and the weights of the intraperitoneally disseminated lesions were measured.

Adverse events. AAV1-sFlt-1 or AAV1 LacZ vectors (2.5×10^{12} genome copies) were injected into the hind limb skeletal muscle of mice. The following experiments were performed to investigate wound healing, neuromuscular damage and body weight changes: Regarding wound healing, a 6-mm square incision was made with scissors in the dorsal skin in nude mice 2 weeks after AAV vector injection, and the healing process was observed with time. As for neuromuscular damage, skeletal muscle of the hind limb at the AAV vector-inoculated site was excised 5 weeks after AAV vector injection, fixed with formalin, paraffin-embedded and sectioned, and the morphology was observed by HE staining. As for body weight changes, body weight of the nude mice was measured before AAV vector injection and 2 and 4 weeks after the administration. Blood was collected 5 weeks after AAV vector injection, and complete blood counts, Alb, BUN, Cr, AST, ALT, Na, K and Cl were measured.

Statistical analysis. Intergroup differences were tested for significance using Student's *t*-test. Survival rates were analyzed by the generalized Wilcoxon and log-rank tests. p values less than 0.05 were considered to be significant.

Results

Detection of VEGF and sFlt-1 in culture supernatants

The concentration of VEGF in the culture supernatant of SHIN-3 cells was 600 pg/ml. sFlt-1 was detected by Western blotting only in the culture supernatant of SHIN-3/sFlt-1 (data not shown).

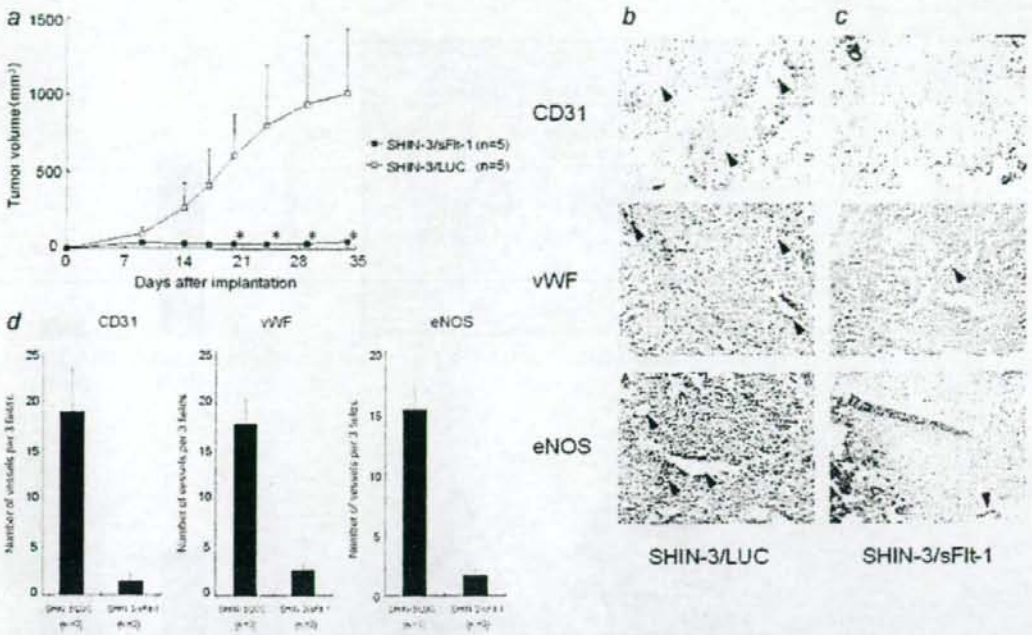

FIGURE 1 – (*a*) *In vivo* tumor growth of sFlt-1-expressing SHIN-3 cells. Tumor cells were subcutaneously injected into the back of mice, and the tumor size was measured every 3 days. The tumor size of SHIN-3/sFlt-1 (■) was significantly smaller than that of SHIN-3/LUC (□, $p < 0.01$ (*)). The tumor volume was calculated using the formula: $(\text{width})^2 \times (\text{length}) \times 0.5$ (mm^3). The data represent the mean ± SD. (*b* and *c*) Immunostaining of subcutaneous tumors of SHIN-3/LUC (*b*) and SHIN-3/sFlt-1 (*c*) with anti-CD31 antibody (upper), anti-vWF antibody (middle) and anti-eNOS antibody (bottom). Endothelial cells of newly formed vessels (arrowhead) were stained dark brown. (*d*) The numbers of new blood vessels in SHIN-3/sFlt-1 and SHIN-3/LUC subcutaneous tumors on the 21st day after inoculation. The number of new blood vessels in SHIN-3/sFlt-1 tumors was significantly smaller than that in SHIN-3/LUC tumors (anti-CD31 antibody; 1.5 ± 0.7 *versus* 19 ± 4, $p < 0.05$, anti-vWF antibody; 2.7 ± 0.6 *versus* 17.7 ± 2.5, $p < 0.01$, anti-eNOS antibody; 1.7 ± 0.6 *versus* 15.3 ± 2.1, $p < 0.01$). Each bar represents the mean ± SD.

In vitro *cell growth kinetics*

The effects of sFlt-1 gene expression on *in vitro* cell growth were examined. There were no differences in growth between SHIN-3/sFlt-1 and the control (SHIN-3/LUC), indicating that the expression of the *sflt-1* gene does not affect *in vitro* cell growth kinetics (data not shown).

Tumor cell transduction model

Subcutaneously inoculated tumor growth. As shown in Figure 1*a*, subcutaneous tumor growth was markedly suppressed in cells expressing sFlt-1. The size of subcutaneous tumors on the 34th day after the transplantation of SHIN-3/sFlt-1 cells was significantly smaller than that of control (43 ± 37 mm^3 *versus* 1004 ± 421 mm^3, $p < 0.01$).

Angiogenesis in subcutaneous tumor. Typical immunohistochemistry of tumors determined using anti-CD31 antibody, anti-vWF antibody and anti-eNOS antibody is shown in Figures 1*b* and 1*c*, and the number of new vessels is summarized in Figure 1*d*. The number of new vessels was significantly smaller in SHIN-3/sFlt-1 than that in control (anti-CD31 antibody; 1.5 ± 0.7 *versus* 19 ± 4, $p < 0.05$, anti-vWF antibody; 2.7 ± 0.6 *versus* 17.7 ± 2.5, $p < 0.01$, anti-eNOS antibody; 1.7 ± 0.6 *versus* 15.3 ± 2.1, $p < 0.01$).

Ascites and peritoneal tumor dissemination. The effects of *sflt-1* gene expression on peritoneal dissemination *in vivo* are shown in Figure 2*a*. The mean volume of ascitic fluid on the 23rd day after intraperitoneal inoculation of SHIN-3/sFlt-1 cells was significantly smaller than that of control (Fig. 2*b*; 0.17 ± 0.13 ml *versus* 1.67 ± 0.71 ml, $p < 0.01$). Similarly, the number of metastasis (Fig. 2*c*) and mean weight of the peritoneally disseminated SHIN-3/sFlt-1 tumors was significantly lower than that of control (Fig. 2*d*; 0.48 ± 0.29 g *versus* 2.74 ± 0.54 g, $p < 0.001$). Thus, *sflt-1* gene expression suppressed ascites production and peritoneal dissemination.

Survival time. The survival of mice was monitored after inoculating tumor cells intraperitoneally. In the control group, the accumulation of ascitic fluid became prominent from the 14th day after inoculation, and all mice died by the 46th day. In contrast, in the SHIN-3/sFlt-1 group, ascitic fluid accumulation was suppressed, resulting in a significantly longer survival (Fig. 2*e*, $p < 0.05$). Therefore, *sflt-1* gene expression prolonged the survival of mice with peritoneal dissemination of ovarian cancer.

Therapeutic model using AAV vector

Serum VEGF concentration and ascitic VEGF concentration. The serum VEGF level was lower than the detection limit in both the subcutaneous and intraperitoneal inoculation groups. In contrast, the ascitic VEGF level was very high (30 ± 9 ng/ml).

Serum sFlt-1 concentration. Following the injection of AAV1-sFlt-1 vector into the mouse skeletal muscles, serum sFlt-1 levels were higher than 1,000 pg/ml throughout the observation period, whereas in the control group with AAV1-LacZ vector, the levels were below the detection limit (Fig. 3*a*).

Tumor growth. The efficacy of muscle-mediated sFlt-1 expression was evaluated in both subcutaneously- and intraperitoneally-transplanted SHIN-3 tumor cell growth. As shown in Figure 3*b*, a

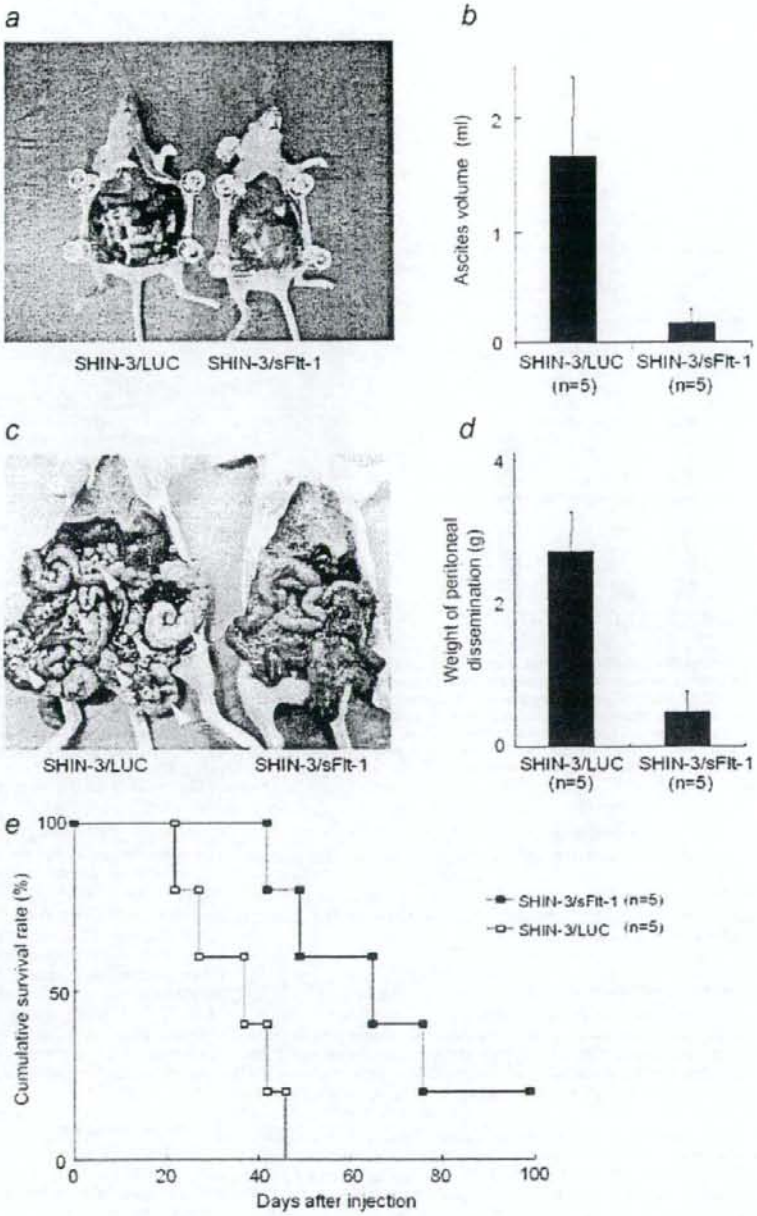

FIGURE 2 – (*a* and *b*) Ascites fluid accumulation on the 23rd day after the intraperitoneal inoculation of cancer cells. Large amounts of bloody ascitic fluid were observed in the SHIN-3/LUC group, whereas in the SHIN-3/sFlt-1 group, the accumulation of ascitic fluid was significantly suppressed (1.67 ± 0.71 ml *versus* 0.17 ± 0.13 ml, $p < 0.01$). (*c* and *d*) Peritoneal dissemination on the 23rd day after peritoneal inoculation of cancer cells. In the SHIN-3/LUC group, marked peritoneal dissemination was observed, particularly on the intestinal surface (arrowheads), whereas in the SHIN-3/sFlt-1 group, peritoneal dissemination was significantly suppressed (2.74 ± 0.54 g *versus* 0.48 ± 0.29 g, $p < 0.001$). (*e*) Kaplan–Meier analysis after intraperitoneal inoculation of cancer cells. Survival was significantly prolonged in the SHIN-3/sFlt-1 group, when compared with that in the SHIN-3/LUC group ($p < 0.05$).

significant suppression of tumor growth was observed in the sFlt-1 injected group ($p < 0.05$). In mice with peritoneal dissemination, the total weight of the peritoneally disseminated lesions on the 23rd day after inoculation was significantly lower than that of control group (Fig. 3*c*; 1.07 ± 0.87 g *versus* 3.15 ± 2.10 g, $p < 0.05$). Therefore, a therapeutic effect was observed in both models.

Survival time. The survival of mice was monitored in both groups. The animals showed accumulation of ascites, and the mean survival lengths were 28.2 and 30.1 days for AAV-LacZ- and AAV-sFlt-1-injected group, respectively. Although the survival in AAV-sFlt-1 group was longer than the controls, statistic significance was not recognized between these groups.

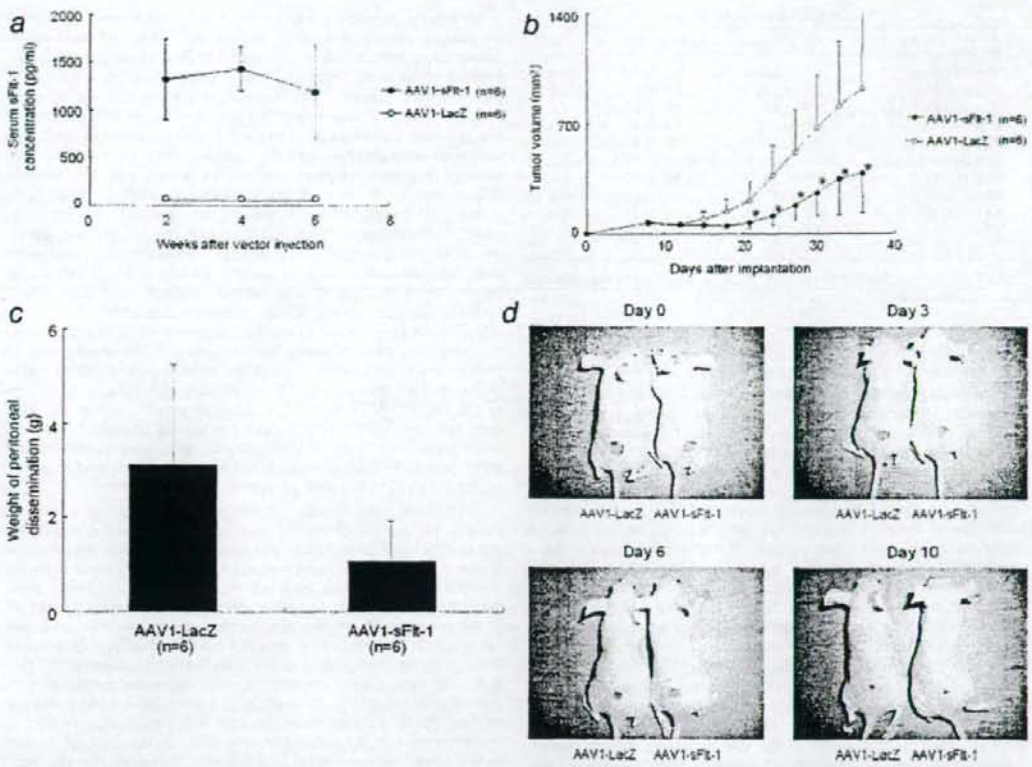

FIGURE 3 – (*a*) Serum sFlt-1 concentrations. In the mice that were intramuscularly injected with AAV1-sFlt-1, the serum sFlt-1 concentration was higher than 1,000 pg/ml. In contrast, in the mice that were intramuscularly injected with AAV1-LacZ, the serum sFlt-1 concentration was below the detection limit. (*b*) Growth of SHIN-3 subcutaneous tumors in the mice that were intramuscularly injected with AAV1-sFlt-1 or AAV1-LacZ. The growth of subcutaneous tumors was significantly suppressed in the intramuscular AAV1-sFlt-1 injection group, compared with that in the intramuscular AAV1-LacZ injection group. The sizes of subcutaneous tumors on the 36th day after the transplantation of SHIN-3 cells in the AAV1-sFlt-1 and AAV1-LacZ groups were 380 ± 250 mm^3 and 921 ± 466 mm^3, respectively (*, $p < 0.05$). (*c*) The total weight of peritoneally disseminated tumors on the 23rd day after the intraperitoneal inoculation of SHIN-3 cells in the mice that had been intramuscularly injected with AAV1-sFlt-1 or AAV1-LacZ. The peritoneal dissemination was significantly suppressed in the AAV1-sFlt-1 group, when compared with that in the AAV1-LacZ group (1.07 ± 0.87 g *versus* 3.15 ± 2.10 g, $p < 0.05$). (*d*) A 6-mm square injury was made in the dorsal region 2 weeks after intramuscular injection of AAV1-sFlt-1 or AAV1-lacZ into nude mice. Photographs of typical views immediately and 3, 6 and 10 days after skin incision are presented. No significant difference was noted between the groups.

Adverse events. Regarding wound healing, the wound was completely repaired about 2 weeks after skin incision in both the AAV1-sFlt-1 ($n = 3$) and control ($n = 3$) groups, showing no significant difference in the time required for healing between the groups. Photographs of typical views immediately and 3, 6, and 10 days after skin incision are shown in Figure 3*d*. As for neuromuscular damage, no apparent damage was noted at the histological level in the AAV1-sFlt-1 group, similar to the control group (data not shown). The body weights were 17.1 ± 1.0, 21.5 ± 0.9, and 23.3 ± 1.2 g before intramuscular AAV vector injection and 2 and 4 weeks after the injection, respectively, in the AAV1-sFlt-1 group ($n = 5$) and 16.9 ± 1.2, 20.7 ± 1.8, and 23.0 ± 1.9 g, respectively, in the control group ($n = 5$), showing no significant difference. The laboratory data are shown in Table I. There were no significant differences in the serum Alb, BUN, Cr, AST, ALT, Na, K or Cl level between the AAV1-sFlt-1 and control groups, nor were there significant differences in the complete blood counts.

Discussion

In this study, we demonstrated the efficacy of muscle-mediated sFlt-1 expression using AAV vectors in both subcutaneous and intraperitoneally disseminated tumors.

A VEGF receptor, Flt-1, consists of an intracellular tyrosine kinase domain, transmembrane domain and extracellular domain, containing 7 immunoglobulin-like domains. sFlt-1 generated by alternative splicing of the Flt-1 gene lacks the intracellular tyrosine kinase and transmembrane domains, and consists of an extracellular domain containing 6 immunoglobulin-like domains, from which the 7th immunoglobulin-like domain is deleted. The VEGF-binding site of Flt-1 is located on the 2nd and 3rd immunoglobulin-like domains in the extracellular domain.[29,30] Hence, sFlt-1 has VEGF-binding ability. However, it has no signal transduction activity because the molecule is not anchored on the cell surface, and lacks the tyrosine kinase do-

TABLE 1 – LABORATORY DATA

	AAV1-LacZ ($n = 3$)	AAV1-sFlt-1 ($n = 3$)	p
WBC (10^3/μl)	1.7 ± 0.3	1.4 ± 0.5	n.s.
Hemoglobin (g/dl)	12.3 ± 1.0	13.9 ± 1.3	n.s.
Platelets (10^4/μl)	75 ± 49	96 ± 42	n.s.
Albumin (g/dl)	0.5 ± 0.1	0.5 ± 0	n.s.
BUN (mg/dl)	36 ± 5	29 ± 4	n.s.
Creatinine (mg/dl)	0.25 ± 0.03	0.19 ± 0.04	n.s.
AST (IU/l)	103 ± 34	86 ± 30	n.s.
ALT (IU/l)	37 ± 5	31 ± 2	n.s.
Na (meq/l)	153 ± 2	154 ± 2	n.s.
K (meq/l)	4.1 ± 0.4	4.2 ± 0.1	n.s.
Cl (meq/l)	116 ± 2	116 ± 2	n.s.

AST, aspartate aminotransferase; ALT, alanine aminotransferase; n.s., not significant.

main. Therefore, sFlt-1 acts as a VEGF antagonist by competing with the original VEGF receptors, Flt-1 and KDR.

Studies suggesting the therapeutic efficacy with sFlt-1-encoding adenoviral vectors for lung[31] or pancreatic[32] cancer have been reported. Our strategy is aimed at attaining long-term sFlt-1 expression not only for tumor suppression but also to prevent the potential recurrence of the tumor after surgical excision. For this purpose, AAV vector appears to be ideal, since transgene expression can be achieved for a number of years.[16,17,24] To date, various serotypes of AAV (1 through 11) have been identified, and the applicability of these serotype-derived vectors has been investigated.[25,33–39] In case of muscle transduction, AAV1-based vector was shown to be more efficient than the rest of the serotypes.[24,25] Therefore, we used AAV1 vectors for *sflt-1* gene transfer. In fact, we had previously attempted the same set of experiments using vectors AAV2 and AAV5; however, none of these experiments showed any promising results (data not shown).

In this study, we confirmed the tumor-suppressive actions of sFlt-1 by transducing tumor cells as we reported in different cell line[14] and demonstrated the therapeutic efficacy of muscle-directed *sflt-1* gene transfer in the tumor-bearing mouse model. Although the muscle transduction model is clinically more relevant, the tumor suppressive action observed in this model was less complete, as assessed by tumor growth (Figs. 1*a vs.* 3*b*), tumor volume (Figs. 2*d vs.* 3*c*) and overall survival. The difference in therapeutic outcome seems to lie in the concentration of sFlt-1 within tumor and the surrounding area. Therefore, in order to obtain more substantial therapeutic benefit, approaches to enhance the supply of sFlt-1 from the muscle by either increasing the vector dose or by transducing more muscle tissues would be necessary. Another approach, increasing the intraperitoneal concentrations of sFlt-1, would be also helpful to improve the therapeutic outcome. However, peritoneal dissemination was inhibited at a concentration of 1,000 pg/ml in this experiment. AAV vectors have an advantage of long-term gene expression, unlike adenovirus vectors, and the level could be maintained at 1,000 pg/ml or higher for as long as 6 weeks in this experiment. The persistent sFlt-1 gene expression may have contributed to the inhibition of peritoneal dissemination. For clinical application, combination of available anticancer drugs and AAV1-sFlt-1 may be recommended more than administration of AAV1-sFlt-1 alone.

Molecular targeted therapy against VEGF has been conducted by using a variety of different molecules.[40–45] Of all these molecules, bevacizumab, an anti-human VEGF monoclonal antibody, appears to be most promising, and clinical trials are ongoing for patients with cancer.[40,42,45] Significant prolongation of progression-free survival was noted in clinical trials with bevacizumab for metastatic colorectal[42] and renal[45] cancer, either in combination with chemotherapy or independently. On the other hand, this strategy requires frequent infusion of drugs, and the adverse effects due to the use of the monoclonal antibody have been noted.[45] Although difficult to predict, our approach may be safer, since it eliminates inherent problems that arise during the repetitive injection of a monoclonal antibody. However, an influence on vascular endothelial cells in normal tissues is a concern as an adverse drug reaction of angiogenesis inhibitors including sFlt-1. Actually, an anti-human VEGF monoclonal antibody, bevacizumab, has been reported to exhibit adverse events of proteinuria, hypertension, nasal bleeding and hematuria.[45] The mechanism of proteinuria is assumed to be injuries of kidney glomerular endothelial and epithelial cells due to bevacizumab-induced reduction of the blood VEGF level.[46] A delay in wound healing has also been reported.[47] However, no delay in wound healing, neuromuscular damage or body weight changes were noted in our experiment, nor were there changes in the laboratory data, and no apparent AAV1-sFlt-1-induced adverse event was observed.

Reports on gene therapy for ovarian cancer that are underway include the use of adenoviral vectors encoding tumor suppressor genes p53[48] and phosphatase and tensin homolog deleted on chromosome 10.[49] These studies aimed at destroying cancer cells by introducing a therapeutic gene into the cancer cells. However, these methods are unrealistic, since introducing a therapeutic gene into all of the peritoneally disseminated cancer cells is impractical. On the other hand, targeted therapy against VEGF is advantageous because it not only has tumor-suppressive effects but also controls the formation of ascites, since it simultaneously suppresses enhanced vascular permeability.[14,50] Theoretically, molecular targeted therapy against VEGF is effective against high VEGF-producing tumors. It is demonstrated that approximately half of the ovarian cancer patients have elevated serum VEGF level.[7] Therefore, this approach would be suitable for at least half of the patients with ovarian cancer. In case of patients who have ovarian cancer with low VEGF-producing tumors, an alternative strategy should be applied. The results of our *in vitro* study suggests that low VEGF-producing ovarian cancer cell lines frequently secrete other angiogenic factors such as PDGF, PD-ECGF and interleukin-8 (unpublished observations). Therefore, a different therapeutic strategy based on the increased level of another angiogenic factor may prove useful for treating patients with low VEGF-producing tumors.

In summary, the experiments using transduced cancer cells confirmed that sFlt-1 has angiogenesis-suppressing activity, through which it inhibits the growth of subcutaneously transplanted ovarian cancer cells and the peritoneal dissemination of tumors. In addition, the *in vivo* experiment that aimed at the clinical application of gene therapy using the AAV vector (AAV1-sFlt-1) revealed that the intramuscular injection of AAV1-sFlt-1 had similar inhibitory effects. These results suggest the possibility of implementing gene therapy using AAV1-sFlt-1 aimed at suppressing peritoneal dissemination of ovarian cancer.

References

1. Jemal A, Tiwari RC, Murray T, Ghafoor A, Samuels A, Ward E, Feuer EJ, Thun MJ. Cancer statistics, 2004. CA Cancer J Clin 2004;54:8–29.
2. Heintz AP. Surgery in advanced ovarian carcinoma: is there proof to show the benefit? Eur J Surg Oncol 1988;14:91–9.
3. McGuire WP, Hoskins WJ, Brady MF, Kucera PR, Partridge EE, Look KY, Clarke-Pearson DL, Davidson M. Cyclophosphamide and cisplatin compared with paclitaxel and cisplatin in patients with stage III and stage IV ovarian cancer. N Engl J Med 1996;334:1–6.
4. Takei Y, Suzuki M, Ohwada M, Saga Y, Kohno T, Machida S, Sato I. A feasibility study of paclitaxel and carboplatin therapy in Japanese patients with epithelial ovarian cancer. Oncol Rep 2003;10: 951–5.
5. Folkman J. Angiogenesis in cancer, vascular, rheumatoid and other disease. Nat Med 1995;1:27–31.
6. Roszkowski P, Wronkowski Z, Szamborski J, Romejko M. Evaluation of selected prognostic factors in ovarian cancer. Eur J Gynaecol Oncol 1993;14 (Suppl):140–5.
7. Cooper BC, Ritchie JM, Broghammer CL, Coffin J, Sorosky JI, Buller RE, Hendrix MJ, Sood AK. Preoperative serum vascular endothelial growth factor levels: significance in ovarian cancer. Clin Cancer Res 2002;8: 3193–7.

8. Davidson B, Goldberg I, Gotlieb WH, Kopolovic J, Ben-Baruch G, Nesland JM, Reich R. The prognostic value of metalloproteinases and angiogenic factors in ovarian carcinoma. Mol Cell Endocrinol 2002; 187(1/2):39–45.
9. Watanabe Y, Nakai H, Ueda H, Nozaki K, Hoshiai H, Noda K. Platelet-derived endothelial cell growth factor predicts of progression and recurrence in primary epithelial ovarian cancer. Cancer Lett 2003;200: 173–6.
10. Sowter HM, Corps AN, Smith SK. Hepatocyte growth factor (HGF) in ovarian epithelial tumour fluids stimulates the migration of ovarian carcinoma cells. Int J Cancer 1999;83:476–80.
11. Kendall RL, Thomas KA. Inhibition of vascular endothelial cell growth factor activity by an endogenously encoded soluble receptor. Proc Natl Acad Sci USA 1993;90:10705–9.
12. Sawano A, Takahashi T, Yamaguchi S, Aonuma T, Shibuya M. Flt-1 but not KDR/Flk-1 tyrosine kinase is a receptor for placenta growth factor (PlGF), which is related to vascular endothelial growth factor (VEGF). Cell Growth Differ 1996;7:213–21.
13. Seetharam L, Gotoh N, Maru Y, Neufeld G, Yamaguchi S, Shibuya M. A unique signal transduction from FLT tyrosine kinase, a receptor for vascular endothelial growth factor VEGF. Oncogene 1995;10:135–47.
14. Hasumi Y, Mizukami H, Urabe M, Kohno T, Takeuchi K, Kume A, Momoeda M, Yoshikawa H, Tsuruo T, Shibuya M, Taketani Y, Ozawa K. Soluble FLT-1 expression suppresses carcinomatous ascites in nude mice bearing ovarian cancer. Cancer Res 2002;62:2019–23.
15. Fisher KJ, Jooss K, Alston J, Yang Y, Haecker SE, High K, Pathak R, Raper SE, Wilson JM. Recombinant adeno-associated virus for muscle directed gene therapy. Nat Med 1997;3:306–12.
16. Kessler PD, Podsakoff GM, Chen X, McQuiston SA, Colosi PC, Matelis LA, Kurtzman GJ, Byrne BJ. Gene delivery to skeletal muscle results in sustained expression and systemic delivery of a therapeutic protein. Proc Natl Acad Sci USA 1996;93:14082–7.
17. Xiao X, Li J, Samulski RJ. Efficient long-term gene transfer into muscle tissue of immunocompetent mice by adeno-associated virus vector. J Virol 1996;70:8098–108.
18. Imai S, Kiyozuka Y, Maeda H, Noda T, Hosick HL. Establishment and characterization of a human ovarian serous cystadenocarcinoma cell line that produces the tumor markers CA-125 and tissue polypeptide antigen. Oncology 1990;47:177–84.
19. Graham FL, Smiley J, Russell WC, Nairn R. Characteristics of a human cell line transformed by DNA from human adenovirus type 5. J Gen Virol 1977;36:59–74.
20. Urabe M, Hasumi Y, Ogasawara Y, Matsushita T, Kamoshita N, Nomoto A, Colosi P, Kurtzman GJ, Tobita K, Ozawa K. A novel dicistronic AAV vector using a short IRES segment derived from hepatitis C virus genome. Gene 1997;200(1/2):157–62.
21. Yoshimura I, Mizuguchi Y, Miyajima A, Asano T, Tadakuma T, Hayakawa M. Suppression of lung metastasis of renal cell carcinoma by the intramuscular gene transfer of a soluble form of vascular endothelial growth factor receptor I. J Urol 2004;171(6, Part 1):2467–70.
22. Wigler M, Pellicer A, Silverstein S, Axel R. Biochemical transfer of single-copy eucaryotic genes using total cellular DNA as donor. Cell 1978;14:725–31.
23. Matsushita T, Elliger S, Elliger C, Podsakoff G, Villarreal L, Kurtzman GJ, Iwaki Y, Colosi P. Adeno-associated virus vectors can be efficiently produced without helper virus. Gene Ther 1998;5:938–45.
24. Mochizuki S, Mizukami H, Kume A, Muramatsu S, Takeuchi K, Matsushita T, Okada T, Kobayashi E, Hoshika A, Ozawa K. Adeno-associated virus (AAV) vector-mediated liver- and muscle-directed transgene expression using various kinds of promoters and serotypes. Gene Ther Mol Biol 2004;8:9–18.
25. Xiao W, Chirmule N, Berta SC, McCullough B, Gao G, Wilson JM. Gene therapy vectors based on adeno-associated virus type 1. J Virol 1999;73:3994–4003.
26. Hermens WT, ter Brake O, Dijkhuizen PA, Sonnemans MA, Grimm D, Kleinschmidt JA, Verhaagen J. Purification of recombinant adeno-associated virus by iodixanol gradient ultracentrifugation allows rapid and reproducible preparation of vector stocks for gene transfer in the nervous system. Hum Gene Ther 1999;10:1885–91.
27. Zolotukhin S, Byrne BJ, Mason E, Zolotukhin I, Potter M, Chesnut K, Summerford C, Samulski RJ, Muzyczka N. Recombinant adeno-associated virus purification using novel methods improves infectious titer and yield. Gene Ther 1999;6:973–85.
28. Kung AL, Wang S, Klco JM, Kaelin WG, Livingston DM. Suppression of tumor growth through disruption of hypoxia-inducible transcription. Nat Med 2000;6:1335–40.
29. Keyt BA, Nguyen HV, Berleau LT, Duarte CM, Park J, Chen H, Ferrara N. Identification of vascular endothelial growth factor determinants for binding KDR and FLT-1 receptors. Generation of receptor-selective VEGF variants by site-directed mutagenesis. J Biol Chem 1996;271:5638–46.
30. Tanaka K, Yamaguchi S, Sawano A, Shibuya M. Characterization of the extracellular domain in vascular endothelial growth factor receptor-1 (Flt-1 tyrosine kinase). Jpn J Cancer Res 1997;88:867–76.
31. Takayama K, Ueno H, Nakanishi Y, Sakamoto T, Inoue K, Shimizu K, Oohashi H, Hara N. Suppression of tumor angiogenesis and growth by gene transfer of a soluble form of vascular endothelial growth factor receptor into a remote organ. Cancer Res 2000;60:2169–77.
32. Hoshida T, Sunamura M, Duda DG, Egawa S, Miyazaki S, Shineha R, Hamada H, Ohtani H, Satomi S, Matsuno S. Gene therapy for pancreatic cancer using an adenovirus vector encoding soluble flt-1 vascular endothelial growth factor receptor. Pancreas 2002;25:111–21.
33. Chiorini JA, Kim F, Yang L, Kotin RM. Cloning and characterization of adeno-associated virus type 5. J Virol 1999;73:1309–19.
34. Chiorini JA, Yang L, Liu Y, Safer B, Kotin RM. Cloning of adeno-associated virus type 4 (AAV4) and generation of recombinant AAV4 particles. J Virol 1997;71:6823–33.
35. Gao G, Vandenberghe LH, Alvira MR, Lu Y, Calcedo R, Zhou X, Wilson JM. Clades of adeno-associated viruses are widely disseminated in human tissues. J Virol 2004;78:6381–8.
36. Gao GP, Alvira MR, Wang L, Calcedo R, Johnston J, Wilson JM. Novel adeno-associated viruses from rhesus monkeys as vectors for human gene therapy. Proc Natl Acad Sci USA 2002;99:11854–9.
37. Mori S, Wang L, Takeuchi T, Kanda T. Two novel adeno-associated viruses from cynomolgus monkey: pseudotyping characterization of capsid protein. Virology 2004;330:375–83.
38. Muramatsu S, Mizukami H, Young NS, Brown KE. Nucleotide sequencing and generation of an infectious clone of adeno-associated virus 3. Virology 1996;221:208–17.
39. Rutledge EA, Halbert CL, Russell DW. Infectious clones and vectors derived from adeno-associated virus (AAV) serotypes other than AAV type 2. J Virol 1998;72:309–19.
40. Cobleigh MA, Langmuir VK, Sledge GW, Miller KD, Haney L, Novotny WF, Reimann JD, Vassel A. A phase I/II dose-escalation trial of bevacizumab in previously treated metastatic breast cancer. Semin Oncol 2003;30(5, Suppl 16):117–24.
41. Garofalo A, Naumova E, Manenti L, Ghilardi C, Ghisleni G, Caniatti M, Colombo T, Cherrington JM, Scanziani E, Nicoletti MI, Giavazzi R. The combination of the tyrosine kinase receptor inhibitor SU6668 with paclitaxel affects ascites formation and tumor spread in ovarian carcinoma xenografts growing orthotopically. Clin Cancer Res 2003;9:3476–85.
42. Kabbinavar F, Hurwitz HI, Fehrenbacher L, Meropol NJ, Novotny WF, Lieberman G, Griffing S, Bergsland E. Phase II, randomized trial comparing bevacizumab plus fluorouracil (FU)/leucovorin (LV) with FU/LV alone in patients with metastatic colorectal cancer. J Clin Oncol 2003;21:60–5.
43. Prewett M, Huber J, Li Y, Santiago A, O'Connor W, King K, Overholser J, Hooper A, Pytowski B, Witte L, Bohlen P, Hicklin DJ. Antivascular endothelial growth factor receptor (fetal liver kinase 1) monoclonal antibody inhibits tumor angiogenesis and growth of several mouse and human tumors. Cancer Res 1999;59:5209–18.
44. Wood JM, Bold G, Buchdunger E, Cozens R, Ferrari S, Frei J, Hofmann F, Mestan J, Mett H, O'Reilly T, Persohn E, Rosel J, et al. PTK787/ZK 222584, a novel and potent inhibitor of vascular endothelial growth factor receptor tyrosine kinases, impairs vascular endothelial growth factor-induced responses and tumor growth after oral administration. Cancer Res 2000;60:2178–89.
45. Yang JC, Haworth L, Sherry RM, Hwu P, Schwartzentruber DJ, Topalian SL, Steinberg SM, Chen HX, Rosenberg SA. A randomized trial of bevacizumab, an anti-vascular endothelial growth factor antibody, for metastatic renal cancer. N Engl J Med 2003;349:427–34.
46. Sugimoto H, Hamano Y, Charytan D, Cosgrove D, Kieran M, Sudhakar A, Kalluri R. Neutralization of circulating vascular endothelial growth factor (VEGF) by anti-VEGF antibodies and soluble VEGF receptor 1 (sFlt-1) induces proteinuria. J Biol Chem 2003;278:12605–8.
47. Niethammer AG, Xiang R, Becker JC, Wodrich H, Pertl U, Karsten G, Eliceiri BP, Reisfeld RA. A DNA vaccine against VEGF receptor 2 prevents effective angiogenesis and inhibits tumor growth. Nat Med 2002;8:1369–75.
48. Zeimet AG, Marth C. Why did *p53* gene therapy fail in ovarian cancer? Lancet Oncol 2003;4:415–22.
49. Saga Y, Mizukami H, Takei Y, Ozawa K, Suzuki M. Suppression of cell migration in ovarian cancer cells mediated by PTEN overexpression. Int J Oncol 2003;23:1109–13.
50. Dvorak HF, Brown LF, Detmar M, Dvorak AM. Vascular permeability factor/vascular endothelial growth factor, microvascular hyperpermeability, and angiogenesis. Am J Pathol 1995;146:1029–39.

JOURNAL OF VIROLOGY, Dec. 2006, p. 11899–11910
0022-538X/06/$08.00+0 doi:10.1128/JVI.00890-06

Vol. 80, No. 24

Induction of Robust Immune Responses against Human Immunodeficiency Virus Is Supported by the Inherent Tropism of Adeno-Associated Virus Type 5 for Dendritic Cells[▽]

Ke-Qin Xin,[1] Hiroaki Mizukami,[2] Masashi Urabe,[2] Yoshihiko Toda,[1] Kaori Shinoda,[1] Atsushi Yoshida,[1] Kenji Oomura,[1] Yoshitsugu Kojima,[1] Motohide Ichino,[3] Dennis Klinman,[4] Keiya Ozawa,[2] and Kenji Okuda[1]*

Departments of Molecular Biodefense Research[1] and Immunology,[3] Yokohama City University Graduate School of Medicine, Yokohama 236-0004, Japan; Division of Genetic Therapeutics, Center for Molecular Medicine, Jichi Medical School, Tochigi-ken 329-0498, Japan[2]; and Center for Biologics Evaluation and Research, U.S. Food and Drug Administration, Bethesda, Maryland 20892[4]

Received 2 May 2006/Accepted 11 September 2006

The ability of adeno-associated virus serotype 1 to 8 (AAV1 to AAV8) vectors expressing the human immunodeficiency virus type 1 (HIV-1) Env gp160 (AAV-HIV) to induce an immune response was evaluated in BALB/c mice. The AAV5 vector showed a higher tropism for both mouse and human dendritic cells (DCs) than did the AAV2 vector, whereas other AAV serotype vectors transduced DCs only poorly. AAV1, AAV5, AAV7, and AAV8 were more highly expressed in muscle cells than AAV2. An immunogenicity study of AAV serotypes indicates that AAV1, AAV5, AAV7, and AAV8 vectors expressing the Env gp160 gene induced higher HIV-specific humoral and cell-mediated immune responses than the AAV2 vector did, with the AAV5 vector producing the best responses. Furthermore, mice injected with DCs that had been transduced ex vivo with an AAV5 vector expressing the gp160 gene elicited higher HIV-specific cell-mediated immune responses than did DCs transduced with AAV1 and AAV2 vectors. We also found that AAV vectors produced by HEK293 cells and insect cells elicit similar levels of antigen-specific immune responses. These results demonstrate that the immunogenicity of AAV vectors depends on their tropism for both antigen-presenting cells (such as DCs) and non-antigen-presenting cells (such as muscular cells) and that AAV5 is a better vector than other AAV serotypes. These results may aid in the development of AAV-based vaccine and gene therapy.

Recombinant adeno-associated viruses (AAVs) have been widely used as gene delivery vectors in animal models (17, 18), and these have entered human clinical trials (34). AAVs have been found in many animal species, including nonhuman primates, canines, fowls, and humans. An increasing number of AAV serotypes have been reported. AAV2, AAV3, and AAV5 are found in humans, while AAV4, AAV7, and AAV8 are found in nonhuman primates (21, 45, 50). The reservoir for AAV1 is unclear because these viruses have not been primarily isolated from tissues; however, reactive antibodies (Abs) against AAV1 have been found to exist in both humans and nonhuman primates (9). AAV6 appears to be a recombinant between AAV1 and AAV2 (60). Most of the current studies involving AAV are based on AAV2 since it was the first available infectious clone (51). The use of AAV2 as a vector to introduce exogenous genes encoding immunogenic proteins for the purpose of vaccination has been explored in several studies conducted by us (65, 66) and other researchers (17, 30, 46, 47). An ex vivo experiment demonstrated that the AAV2 vector can transduce dendritic cells (DCs) and that these cells then present the AAV-encoded antigen to T cells (46, 65). Other AAV serotypes may have advantages as vaccine vectors because AAV serotypes differ in their tissue and/or cell tropism (23, 25, 30, 47). For example, AAV1 and AAV7 are more efficient than AAV2 for the transduction of skeletal muscle (21, 60), while AAV3 is superior for the transduction of megakaryocytes (27). AAV5 and AAV6 infect apical airway cells more efficiently (24, 68). AAV2, AAV4, and AAV5 infect cells of the central nervous system; however, differences with regard to the distribution and target cell types exist among these three serotypes (68).

AAV is a small, single-stranded DNA virus that lacks an envelope. This virus requires a helper virus to facilitate efficient replication. The genome of wild-type AAV is known to integrate into the human genome at a specific site on chromosome 19q (36). However, in nondividing cells, AAV vector genomes mostly adopt the form of concatameric circular episomes that comprise active transcriptional units (16, 54). AAV is currently the only nonpathogenic viral vector that has been shown to mediate long-term gene expression without causing toxicity in vivo. Using this vector system, exogenous genes have been efficiently transferred into a number of tissues, including brain (18), muscle (29), lung (19), gut (17), liver (55), and eye (37). A human clinical trial of AAV2 has been conducted (34, 41).

The objectives of the present study were (i) to compare the immunogenicities of AAV serotypes (1 to 8) expressing human

* Corresponding author. Mailing address: Department of Molecular Biodefense Research, Yokohama City University Graduate School of Medicine, 3-9 Fukuura, Kanazawa-ku, Yokohama 236-0004, Japan. Phone: 81(45)787-2602. Fax: 81 (45)787-2851. E-mail: kokuda@med.yokohama-cu.ac.jp.

▽ Published ahead of print on 27 September 2006.

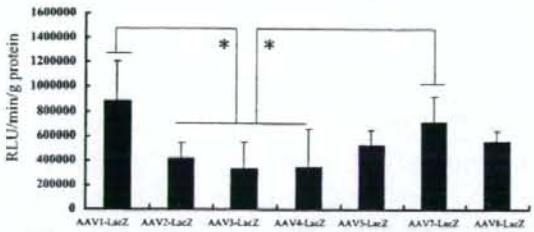

FIG. 1. Transduction of mouse muscle by AAV serotype vectors. AAV LacZ-expressing vectors (10^{10} vp) were injected intramuscularly into five mice/group. β-Galactosidase activity in the muscle was examined 2 weeks later using the Beta-Glo Assay System. An asterisk indicates a significant difference between the two groups ($P < 0.05$). RLU, relative light units.

immunodeficiency virus (HIV) Env gp160 in BALB/c mice, (ii) to compare the immunogenicities of AAV serotype vectors produced by HEK293 cells and insect cells, and (iii) to evaluate the mechanisms involved in the observed responses.

MATERIALS AND METHODS

AAV production. AAV vectors were generated as described previously (65, 66). In brief, a *lacZ* gene or a fragment containing HIV Env gp160 and Rev coding genes, which were derived from the HIV IIIB strain, was subcloned into a shuttle vector containing the cytomegalovirus (CMV) promoter, poly(A), and the AAV2 inverted terminal repeat (the AAV5 inverted terminal repeat was used for construction of the AAV5 vector; the AAV2 inverted terminal repeat was used for other AAV serotype vectors). We included a Rev coding gene in the construct because expression of HIV Env gp160 is dependent on Rev protein. This approach resulted in increased HIV Env gp160 protein expression in vitro and enhanced immune responses against HIV Env gp160 in vivo (33). The recombinant shuttle vector was packaged by triple transfection of HEK293 cells with an adenovirus helper plasmid, a chimeric packaging construct in which the AAV2 Rep gene was fused to the cap gene derived from either AAV serotype, and a shuttle vector plasmid to produce pseudotypes AAV2-based AAV1-LacZ, AAV2-LacZ, AAV3-LacZ, AAV4-LacZ, AAV5-LacZ, AAV7-LacZ, and AAV8-LacZ or AAV1-HIV, AAV2-HIV, AAV3-HIV, AAV4-HIV, AAV5-

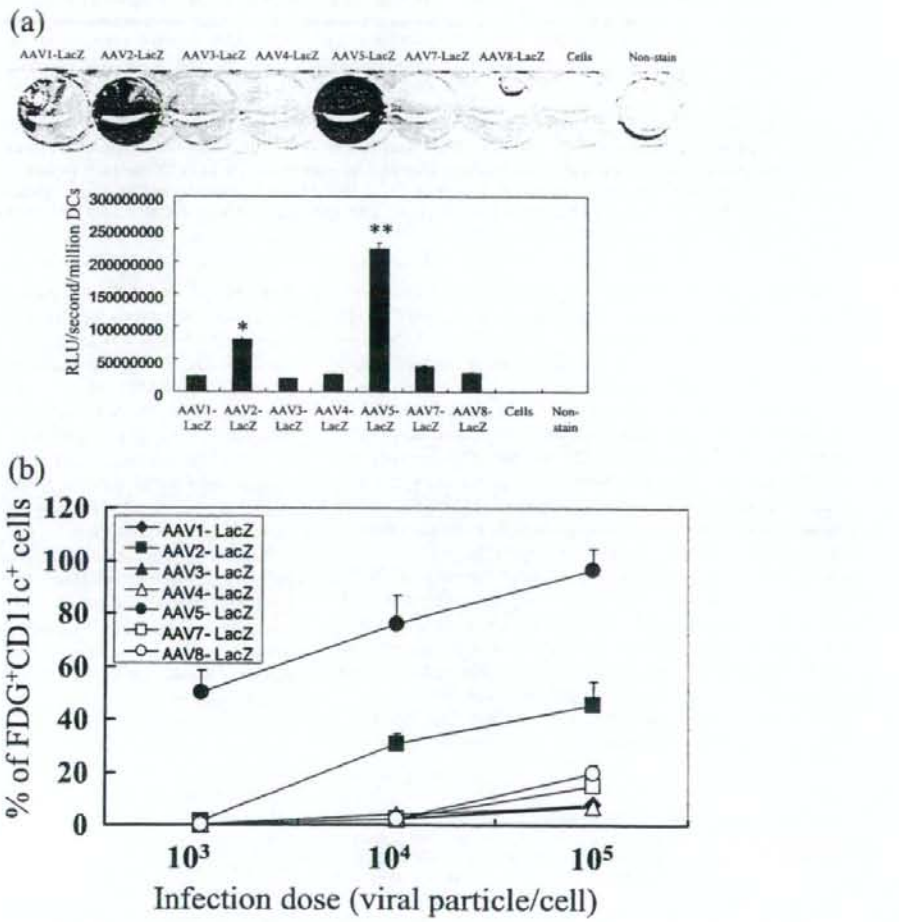

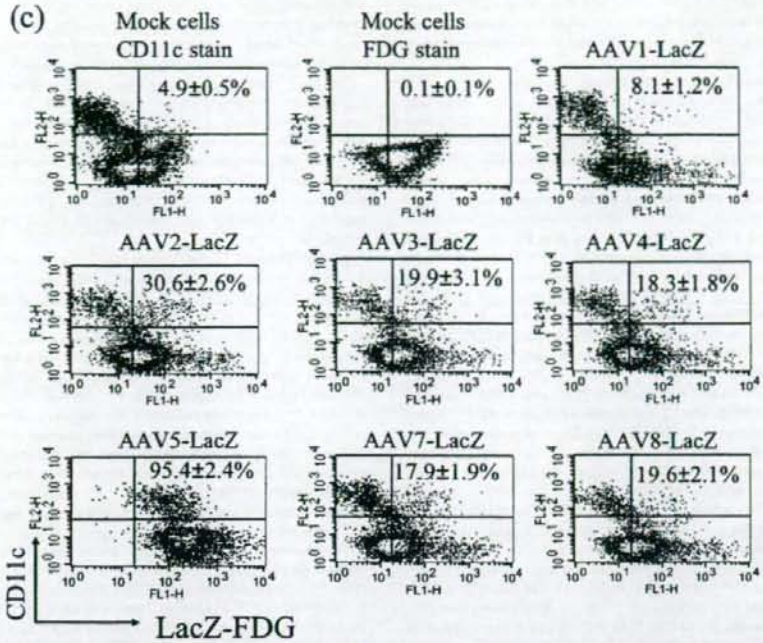

FIG. 2. Transduction of mouse purified DCs by AAV serotype vectors. (a) Mouse CD11c$^+$ DCs were transduced with LacZ-expressing AAV vectors at 10^4 vp/cell (triplicate for each sample). Two days after infection, the cells were stained with X-Gal (upper panel), and the β-galactosidase activity was measured using the Beta-Glo Assay System (bottom panel). The data presented were averaged from three separate experiments. The asterisk indicates a significant difference when AAV2-LacZ-transduced cells were compared to AAV1-LacZ-, AAV3-LacZ-, AAV4-LacZ-, AAV7-LacZ-, and AAV8-LacZ-transduced cells and mock-transduced cells; the double asterisk indicates a significant difference when AAV5-LacZ-transduced cells were compared to AAV2-LacZ-transduced cells. RLU, relative light units. (b) Mouse CD11c$^+$ DCs were transduced with AAV-LacZ vectors at 10^3 to 10^5 vp/cell (triplicate for each sample). Two days after transduction, the cells were stained with X-Gal, and the percentages of LacZ-expressing DCs (FDG$^+$ CD11c$^+$ DCs) were determined. The data presented were averaged from three separate experiments. (c) Enriched immature DCs were transduced with 10^5 vp/cell of various AAV-LacZ vectors (triplicate for each sample). Two days after transduction, the cells were treated with PE-conjugated anti-mouse CD11c Ab and FDG followed by flow cytometric analysis. The data provided represent the fraction of FDG/CD11c dual-positive cells as a percentage of the total population of CD11c$^+$ cells. The data presented were averaged from three independent experiments.

HIV, AAV7-HIV, and AAV8-HIV vectors. The AAV vectors were purified by the standard cesium chloride sedimentation method (65, 66). The titer was determined by quantitative DNA dot blot hybridization.

The insect cell-produced AAV vectors (BacAAVs) were generated as described previously (58). The fragment containing the CMV promoter, HIV Env gp160 and Rev coding genes, and poly(A) was excised from the AAV shuttle vector by using NotI; the resulting fragment was inserted into the corresponding site of a baculovirus transfer plasmid between the serotype 2 or 5 inverted terminal repeats. Recombinant baculoviruses were generated by using the Bac-to-Bac baculovirus expression system (Invitrogen, Carlsbad, CA). Recombinant baculoviruses containing the HIV Env gp160 and Rev coding genes; an AAV Rep of serotypes 1, 2, and 5; and an AAV1, AAV2, or AAV5 capsid were used to infect insect cells in order to produce BacAAV1-HIV, BacAAV2-HIV, and BacAAV5-HIV vectors, respectively. The AAV vectors produced were purified by two rounds of ultracentrifugation with a standard cesium chloride density gradient (65, 66). The titer was determined by quantitative DNA dot blot hybridization.

In vivo expression of β-galactosidase. The AAV-LacZ vector (10^{10} viral particles [vp]/mouse) was injected into mouse muscle. Two weeks after the administration, the mouse was sacrificed and the β-galactosidase activity in the muscle was monitored periodically from 1 week through 6 months after administration by using the Beta-Glo Assay System (Promega, Madison, WI).

Mouse DC preparation. DCs were isolated from BALB/c mouse bone marrow, as described previously (7, 62). In brief, the bone marrow was obtained from the tibia and femur of BALB/c mice. The DCs at a density of 5×10^5 cells/ml were cultured in RPMI 1640 medium containing 10% fetal calf serum, 1 ng/ml recombinant granulocyte-macrophage colony-stimulating factor (GM-CSF; Kirin Beer Corp., Tokyo, Japan), and recombinant interleukin-4 (IL-4) for 6 days.

Transduction of AAV vectors to mouse cells. Immature mouse DCs were stained with phycoerythrin (PE)-conjugated anti-mouse CD11c antibody (clone N418; eBioscience, Boston, MA). The CD11c$^+$ DCs were sorted using a MoFlo Cell Sorter (Takara Bio Corp., Tokyo, Japan). The cells were transduced with LacZ-expressing serotype AAV vectors at 37°C at 10^3 to 10^5 vp/cell for 2 days. The transduced cells were washed with phosphate-buffered saline (PBS) and stained with 40 mM X-Gal (5-bromo-4-chloro-3-indolyl-β-D-galactopyranoside) in staining buffer [5 mM $K_3Fe(CN)_6$, 5 mM $K_4Fe(CN)_6$, 2 mM $MgCl_2$ in PBS] at 37°C for 2 h. The β-galactosidase activity was detected by using the Beta-Glo Assay System (Promega). To count LacZ-expressing cells, the sorted CD11c$^+$ DCs were treated with 1 μM of fluorescein digalactoside (FDG; Molecular Probes, Eugene, OR) followed by flow cytometric analysis (the data are shown in Fig. 2b). The enriched, unsorted DCs were transduced with LacZ-expressing serotype AAV vectors at 37°C at 10^5 vp/cell for 2 days. The cells were stained with anti-mouse CD11c antibody and treated with FDG followed by flow cytometric analysis (the data are shown in Fig. 2c).

The mouse DCs used in this study were derived from GM-CSF- and IL-4-treated bone marrow cells. To explore the efficiencies of transduction of AAV serotype vectors to hematopoietic cells, unpurified mouse splenocytes and bone marrow cells were transduced with LacZ-expressing serotype AAV vectors at 10^5 vp/cell at 37°C for 2 days. The bone marrow cells were treated with 1 μM of FDG, and splenocytes were treated with 1 μM of FDG and PE-conjugated